1. Report No.	2. Government Accession No.	3. Recipient's Catalog No.

4. Title and Subtitles	5. Report Date
Characterization, Evaluation and Implementation of Fiber Reinforced Polymer Composites for Highway Infrastructure	
	6. Performing Organization Code

7.Authors	8. Performing Organization Report No.
Srinivas Aluri, Roger Chen, Jacky Prucz, Eung Cho, Robert Creese, Hota Gangarao, Rakesh Gupta, Udaya Halabe, Samer Petro, Powsiri Klinkhachorn, Ruifeng Liang, Vimala Shekar, Hema Siriwardane and P.V.Vijay	

9. Performing Organization Name and Address.	10. Work Unit No. (TRAIS)
West Virginia University Research Corporation-Office of Sponsored Programs Constructed Facilities Center 886 Chestnut Ridge Road Morgantown, WV 26506-6845	
	11. Contract or Grant No. DTFH61-01-R-00002

12. Sponsoring Agency Name and Address	13. Type of Report and Period of Covered
Federal Highway Administration Office of Acquisition Management HAAM-20A, Room 4410 Washington, D.C.20590	Draft Final Report 8/9/2001 – 4/8/2004
	14. Sponsoring Agency Code

15. Supplementary Notes

16. Abstract

This research is divided into five sections: characterization, evaluation, implementation, cost-analysis and reporting. The section on characterization involves designing, characterizing and evaluating the relationships of FRP composites by modifying resin systems (composition, additives including nanoclays, structure, process etc.), fabrics (3-D stitched and braided fabrics with appropriate sizings) and manufacturing techniques (resin transfer molding, pultrusion, compression molding etc.). Stitched fabric composites' behavior was studied and modeled. Performance of geosystems with silty soils and drainage and consolidation properties of reinforced soils was investigated. The section on structural evaluation includes increasing sensitivity of the infrared thermography technique by investigating the use of image processing in the frequency domain and the use of fuzzy logic/neural network based data interpretation methodologies. In addition, the research includes the setup of microbending and optical reflectometer laboratory instrumentation for defect detection and qualitative mapping of stresses in the FRP specimens. Vibration signatures presently being studied for damage detection in actual structures were used, by extending the 1-D (beam) strain energy based damage detection algorithm to develop damage detection algorithms for 2-D (plate) systems. Using AE signals, material constants and the fracture parameters will be correlated to determine the structural integrity of the FRP plates, and the time and capacity of the final failure will be predicted. The section on implementation involves studying the performance levels (stiffness and strength) of an FRP modular deck-steel stringer system under AASHTO HS-25 design loads including fatigue, monitoring the performance of connections between module-to-module and deck-to-stringer at a system level, and recommending design steps for bridge superstructure with FRP modular decks. Structural performance of the system (FRP deck with supporting stringers) was evaluated in the laboratory under static and fatigue loading in terms of: deflection, effective flange width, transverse load distribution factor, flexural rigidity, degree of composite action, and ultimate strength of an FRP bridge deck system. The cost analyses section includes developing a database for evaluating maintenance, repair, and rehabilitation costs of FRP bridge decks and comparing these costs to those associated with traditional bridge decks. In particular, PACES (Parametric Cost Engineering System) program developed by the U.S. Air Force for evaluating repair/rebuild structural alternatives was used for accomplishing the objectives of this task. Data from PACES was compared with WVDOH and other State Highway Departments including the evaluation of new materials (such as wraps) for rehabilitation in terms of life extensions obtained from such materials. The final section deals with the preparation of the final report and submittal to COTRFHWA.

17. Key Words	18. Distribution Statement
	No restrictions.

19. Security Classif. (of this report)	20. Security Classif. (of this page)	21. No. of Pages	22. Price
Unclassified	Unclassified		

Task 5.3.3: Performance of Polymer Concrete Wearing Surfaces on FRP Decks

Ruifeng Liang

Abstract

At least 175 vehicular bridges and 161 pedestrian bridges are in service worldwide that utilized fiber reinforced polymer (FRP) composites. 83 out of 135 vehicular bridges in the United States have employed FRP composite bridge deck systems while others have used FRP rebars, tendons, structural shapes including flat panels. The repaid growth of FRP composites for bridge applications is attributed to market acceptance and public recognition in terms of superior performance, durability, corrosion resistance and high strength to weight ratio in comparison with steel. The FRP decking systems are usually bonded with polymer concrete as wearing surface in the field for proper traction and rideability. However, cracking of polymer concrete wearing surface mostly along the length of a joint connecting FRP modules in the field has been noted in several FRP bridge deck systems. Similarly, delamination of polymer concrete from FRP decks has been observed in very few bridges. Durability of the wearing surface appears to be the principal maintenance issue. The focus of this study is to evaluate different commercially available polymer concrete (PC) overlay systems for their applicability and durability over FRP deck systems.

Three representative resin binders were selected for this investigation, including 1) Poly-Carb Flexogrid Mark-163, a urethane modified epoxy co-polymer system; 2) Transpo Industries T-48, a low modulus, polysulfide modified epoxy system; and 3) E-Bond Epoxies 526, a flexible, low modulus epoxy resin system. Experimental studies on these resin binders and their polymer concrete systems with reference to FRP deck panels included: 1) measurements of coefficient of thermal expansion for their thermal compatibility between PC overlay and FRP deck; 2) characterization of strain compatibility at the interface of PC overlay and FRP deck; and 3) determination of bond strength at the interface, with emphasis on the most effective surface preparation method.

It is concluded that T-48 overlay system and E-Bond 526 overlay system have better thermal compatibility with FRP deck than Poly-Carb 163. E-Bond 526, however, appears to have the best strain compatibility at the interface with FRP deck, which is followed by T-48 and then Poly Carb Mark-163. Again, T-48 overlay system presents an excellent bond strength that is 120% higher than that of E-Bond 526 or 15% higher than that of PolyCarb Mark –163. As a result of this study, Transpo T-48 is identified to be the most compatible overlay system for glass FRP deck applications. Poly-Carb Mark 163 has significant advantages over E-Bond 526 in the sense of bond strength and energy absorption capacity, whereas E-Bond 526 has exhibited better thermal and strain compatibility at the interface of PC and FRP deck than Poly-Carb Mark 163.

It is also concluded that a very fine grit sanding and proper cleaning is sufficient to yield good bond strength and a coarser grit sanding does not necessarily give better bond strength. With a fine grit sanding, the bond strengths for three resin binders are: 1800 psi with T-48, 1570 psi with Polycarb, and 850 psi with E-Bond. As compared to the results from grit paper sanding method, the peel-ply method gives much lower bond strength but presents some field-operation advantages due to ease of use and the ability to get a good even preparation. With a medium peel-ply, the bond strengths are 880 psi for Poly-Carb, 840 psi for T-48, and 670 psi for E-Bond. Whether these bond strengths are sufficient enough to avoid premature failure has to be addressed.

The experimental results were further discussed with reference to field observations of existing wearing surfaces on three FRP bridges: 1) Market Street bridge, Wheeling, WV, constructed in July 2001; 2) Katy Truss bridge, Fairmont, WV, constructed in July 2001; and 3) La Chein bridge, Monroe County, WV, constructed in August 2002. All three FRP bridge decks have used a 3/8-inch thin polymer concrete overlay. The wearing surface of Market Street bridge using Poly-Carb Mark 163 has thus far performed extremely well. However, the wearing surfaces on Katy Truss bridge using Poly-Carb Mark 163 and La Chein bridge using Transpo T-48 had debonding problems. As compared to well-controlled conditions in the laboratory, the field environmental conditions are highly complicated, resulting in continued field evaluation of this study.

The author would like to thank Dr Michael Sprinkel for valuable comments and U.S. DOT/FHWA for its funding in this work. The author also thanks resin binder suppliers for providing materials used under this investigation.

TABLE OF CONTENTS

ABSTRACT ii

TABLE OF CONTENTS iv

LIST OF FIGURES viii

LIST OF TABLES x

1. INTRODUCTION

1.1 Background 1

1.2 Objective 3

1.3 Materials Investigated 4

1.4 Scope 4

2. LITERATURE REVIEW

2.1 Introduction 5

2.2 The Past 25 Years' Polymer Concrete Practice 5

2.2.1 Overlay Materials 5

2.2.2 Construction Methods 6

2.2.3 Performance 11

2.2.4 Cost 11

2.3 Past Evaluations 11

2.3.1 Material Description 12

2.3.2 Experimental Program 12

2.3.2.1 Coupon Testing 12

2.3.2.2 Beam Testing 12

2.3.3 Evaluation of Data 13

2.3.4 Field Placement 13

2.3.5 Review 14

2.4 Conclusion 14

3. COEFFICIENT OF THERMAL EXPANSION TESTING

3.1 Introduction 15

3.2 Specimen Preparation 15

3.3 Test Method 15

3.4 Results 17

3.5 Discussion & Conclusions 20

4. DEVELOPMENT OF STRAIN VARIATION DIAGRAM

4.1 Introduction 22

4.2 Specimen Preparation 22

4.3 Test Method 23

4.4 Results 24

4.5 Discussion & Conclusions 26

5. BOND STRENGTH TESTING

5.1 Introduction 28

5.2 Specimen Preparation 28

5.3 Test Method 30

5.4 Results 31

5.5 Discussion & Conclusions 32

6. FIELD OBSERVATIONS

6.1 Introduction 35

6.2 Problems In The Field 35

6.2.1 Katy Truss Bridge 36

6.2.2 La Chein Bridge 37

6.2.3 Market Street Bridge 40

6.3 Discussions & Conclusions 43

7. CONCLUSIONS & RECOMMENDATIONS

7.1 Introduction 45

7.2 Conclusions 45

7.3 Recommendations 46

BIBLIOGRAPHY 47

APPENDICES

A. BENDING TEST OF FRP PANELS WITH PLANT CAST WEARING SURFACES

A.1 Introduction 51

A.2 Specimen Preparation and Test Method 51

A.3 Results 52

A.3.1 Variable Peel-Ply Roughness 52

A.3.1.1 Fine Grade 52

A.3.1.2 Medium Grade 53

A.3.1.3 Rough Grade 54

A.3.2 Vinyl Ester Binder 56

A.3.2.1 Basaltic Aggregate 56

A.3.2.2 Quartz Aggregate 57

A.4 Conclusions 58

B. RAW TEST DATA

B.1 Coefficient of Thermal Expansion Data 59

B.2 Strain Variation Diagram Data 64

B.3 Bond Strength Data 66

C. ASTM STANDARDS FOR POLYMERS AND POLYMER CONCRETE 68

D. CONTACT INFORMATION FOR POLYMER CONCRETE OVERLAY SUPPLIERS 69

LIST OF FIGURES

Figure 1.1.1:	A FRP Composite Bridge –Market Street Bridge.	2
Figure 1.1.2:	Schematic of A Polymer Concrete Wearing Surface.	2
Figure 3.3.1:	Specimen schematic for CTE measurement.	16
Figure 3.4.1:	The thermal expansion (microstrain) versus temperature data for Polycarb Mark-163 resin binder.	17
Figure 3.4.2:	The thermal expansion (microstrain) versus temperature data for Polycarb Mark-163 polymer concrete.	18
Figure 3.4.3:	The thermal expansion (microstrain) versus temperature data for Transpo T-48 resin binder.	18
Figure 3.4.4:	The thermal expansion (microstrain) versus temperature data for Transpo T-48 polymer concrete.	19
Figure 3.4.5:	The thermal expansion (microstrain) versus temperature data for E-Bond 526 resin binder.	19
Figure 3.4.6:	The thermal expansion (microstrain) versus temperature data for E-bond 526 polymer concrete.	20
Figure 4.2.1:	Specimen schematic for strain variation diagram measurement	23
Figure 4.4.1:	Strain variation diagram for Polycarb Mark-163	24
Figure 4.4.2:	Strain variation diagram for Transpo T-48	25
Figure 4.4.3:	Strain variation diagram for E-Bond 526	25
Figure 5.2.1:	Specimen preparation and dimensions	29
Figure 5.3.1:	Schematic of test setup	30
Figure 5.4.1:	Bond stress vs. surface preparation level using various grit of sanding papers	31

Figure 5.4.2:	Bond stress vs. surface preparation level using various peel-plies	32
Figure 6.2.1.1:	Delamination of the wearing surface on the Katy Truss Bridge.	36
Figure 6.2.1.2:	Delamination of FRP mat used to reinforce the field joint on Katy Truss Bridge.	37
Figure 6.2.2.1:	A crack located on La Chein Bridge.	38
Figure 6.2.2.2:	Close up of a crack on La Chein Bridge.	38
Figure 6.2.2.3:	Cracking and delamination on La Chein Bridge.	39
Figure 6.2.2.4:	Cracking and delamination on La Chein Bridge.	39
Figure 6.2.2.5:	Location of cracks on La Chein Bridge.	40
Figure 6.2.3.1:	Crack locations and sizes on Market Street Bridge section 1.	41
Figure 6.2.3.2:	Crack locations and sizes on Market Street Bridge section 2.	42
Figure 6.2.3.3:	Surface Cracks in PC overlay, Market Street Bridge.	42
Figure 6.2.3.4:	Surface Cracks in PC overlay, Market Street Bridge.	43
Figure A.3.1.1.1:	Strain variation diagram for fine peel-ply.	53
Figure A.3.1.2.1:	Strain variation diagram for medium peel-ply.	54
Figure A.3.1.3.1:	Strain variation diagram for rough peel-ply.	55
Figure A.3.2.1.1:	Strain variation diagram for basaltic aggregate.	56
Figure A.3.2.2.1:	Strain variation diagram for quartz aggregate.	57

LIST OF TABLES

Table 2.2.1.1:	Characteristics of some polymer concrete overlay binders.	7
Table 3.5.1:	Coefficients of thermal expansion of polymer binders and concretes investigated	21
Table 7.2.1	Summary of results	46
Table A3.1.1.1:	Strain data for fine grade peel-ply bending test.	52
Table A3.1.2.1:	Strain data for medium grade peel-ply bending test.	53
Table A3.1.3.1:	Strain data for rough grade peel-ply bending test.	54
Table A3.2.1.1:	Strain data for vinyl ester binder with basalt aggregate, bending test.	56
Table A3.2.2.1:	Strain data for vinyl ester binder with quartz aggregate, bending test.	57
Table B.1.1:	Raw CTE data for Polycarb Mark 23 neat resin.	59
Table B.1.2:	Raw CTE data for Polycarb Mark 23 polymer concrete.	60
Table B.1.3:	Raw CTE data for Transpo T-48 neat resin.	61
Table B.1.4:	Raw CTE data for Transpo T-48 polymer concrete.	62
Table B.1.5:	Raw CTE data for E-Bond 526 neat resin.	63
Table B.1.6:	Raw CTE data for E-Bond 526 polymer concrete.	64
Table B.2.1:	Strain data for Polycarb Mark 23.	64
Table B.2.2:	Strain data for Transpo T-48.	65
Table B.2.3:	Strain data for E-Bond 526.	65
Table B.3.1:	Bond strength data for Polycarb Mark 23.	66
Table B.3.2:	Bond strength data for Polycarb Mark 23 with peel ply surface preparation.	66
Table B.3.3:	Bond strength data for Transpo T-48.	66

Table B.3.4: Bond strength data for Transpo T-48 with peel ply surface preparation. 67

Table B.3.5: Bond strength data for E-Bond 526. 67

Table B.3.6: Bond strength data for E-Bond 526 with peel ply surface preparation. 67

1. INTRODUCTION

1.1 Background

Fiber reinforced polymer (FRP) composites are promoted as the 21st century materials and are being accepted as replacements of traditional materials in many applications (Stewart, 2002; Moretti, et al., 2002). The main reasons for such acceptance are: 1) higher specific strength and stiffness than steel or wood; 2) higher fatigue strength and impact energy absorption capacity; 3) better resistance to corrosion (non-conductive), rust, fire, hurricane, ice storm, acids, water intrusion, temperature changes, attacks from micro-organisms, insects, and woodpeckers; 4) longer service life (over 80 years); 5) lower installation, operation and maintenance costs; and 6) consistent batch-to-batch performance.

Advances in FRP composite products have lead to structural systems that allow for repaid deployment of bridge decks and other highway structures. The Market Development Alliance of the FRP Composites Industry has recently published a report on global FRP use for bridge applications. According to that report, at least 175 vehicular bridges and 161 pedestrian bridges are in service worldwide that utilized fiber reinforced polymer (FRP) composites (MDA, 2003). 83 out of 135 vehicular bridges in the United States have employed FRP composite bridge deck systems while others have used FRP rebars, tendons, structural shapes including flat panels. Figure 1.1.1 is a photo of Market Street Bridge, Wheeling, West Virginia where FRP decks were supported by on steel girders and covered with a polymer concrete wearing surface.

All bridge deck systems require either an applied wearing surface or the wearing surface being part of the deck itself as in the case of concrete bridge decks. Wearing surface is the first line of defense in combating environmental and traffic related degradation of bridge decks and superstructures. In addition, wearing surfaces, also termed as overlays, provide a nonskid traffic surface and sufficient geometric tolerances including crown to run rain water off the deck without logging problem. A wearing surface can be constructed with a conventional latex concrete or high-density concrete, or a hot- applied asphalt, or a polymer concrete. For FRP bridge decks, both 2-inch thick conventional asphalt overlays and 3/8-inch thin polymer concrete overlays have been frequently used in field (Ralls, 2004; FHWA, 2001; FHWA, 2003; Justice, 2004; Reeve, et al., 2004; Yannotti, et al., 2004; Deitz, 2002; Solomon, 2002).

Figure 1.1.1 A FRP Composite Bridge - Market Street Bridge (Wheeling, West Virginia, Constructed in July 2001)

In order to utilize the full advantages of FRP bridge decks, a thin polymer concrete overlay should be selected for FRP deck applications (Cassity, 2002; Scott, et al., 2001)). First of all, 2-inch thick conventional overlays will add significant amount of dead weight onto the decking system. Furthermore, a conventional latex concrete or high-density concrete does not have comparable stiffness and strength properties or thermal properties as compared to FRP deck systems, while a hot-applied asphalt overlay should not be used either because the typical asphalt temperature exceeds the glass transition temperature of the polymer resin used in the FRP decks

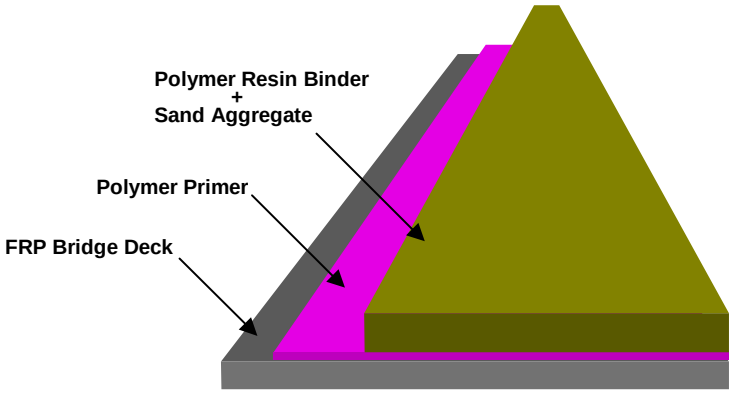

Figure 1.1.2 Schematic of A Polymer Concrete Wearing Surface

Polymer concrete overlay systems are usually comprised of a polymer primer, a polymer resin binder, and dry sand aggregate, as schematically shown in Figure 1.1.2. The primer's main function is to enhance the bond between the FRP deck and the polymer concrete. There are several polymer concrete overlay systems available in the market for bridge decks (see AASHTO SHRP 2035B, 1999; AASHTO, 1995). However, those overlay systems still need to be evaluated for their applicability to FRP decks prior to field application, because those systems were originally formulated for conventional concrete or steel bridge decks (ASTM C881; ACI 548.5R). FRP composites have very different thermo-mechanical properties from those of concrete or steel. For example, epoxy-based overlay systems have much better bonding strength with concrete decks than that with FRP decks, leading to different failure patterns.

Many FRP bridges with polymer concrete wearing surfaces have been performing satisfactorily (Black, 2003; Justice, 2004). However, delamination and/or cracking of polymer concrete wearing surface in the field has been noted in several FRP bridge deck systems (Justice, 2004; FHWA 2003; Yannotti et al 2004;). Durability of the wearing surface appears to have become a principal maintenance issue. Such cracking or delamination may be attributed to possible incompatibilities in the thermo-mechanical response of polymer concrete wearing surface with the substrate (FRP composites deck). Each polymer has different mechanical response (subjected to a loading) and different thermal response (subjected to a temperature change). Lack of compatibility in thermo-mechanical properties between the deck and overlay, due to different polymers, can lead to debonding and/or cracking of the overlay. Delamination or cracking of polymer concrete over a FRP deck may also occur due to poor adhesion (i.e., weak interfaces) between the polymer concrete and FRP deck. Adequate surface preparation is particularly important for the effective bonding of polymer concrete to the composite deck.

The focus of this study is to evaluate different commercially available polymer concrete (PC) overlay systems for their applicability and durability over FRP deck systems.

1.2 Objectives

The objective of this work was to compare the usability of several commercially available polymer concrete overlay systems and determine an optimal surface preparation method for use with modular FRP composite bridge deck systems developed at Constructed Facilities Center, West Virginia University.

1.3 Materials Investigated

Three commercial resin binders were used in this investigation. Polycarb Flexogrid Mark-163 is urethane modified epoxy co-polymer system. The mixing ratio for its two components (Part A and Part B) is 2:1 by volume. Transpo T-48 is a low modulus, polysulfide modified epoxy and also has a mixing ratio of 2:1 by volume for Part A and Part B. E-Bond 526 is a flexible, low modulus, 100% solids, two component epoxy resin system with a mixing ratio of 1:1 by volume.

1.4 Scope

The scope of work includes 1) evaluation and comparison of the above commercially available polymer concrete overlay systems in terms of the following thermal-mechanical properties: i) Coefficient of Thermal Expansion (CTE); ii) bending strain compatibility; and iii) bond strength; and 2) determination of the optimal surface preparation by establishing the relationship between bond strength and the level of surface preparation, and the most practical method of surface preparation by comparing the sanding method with a commercial peel-ply system.

2. LITERATURE REVIEW

2.1 Introduction

The need for a suitable wearing surface has been around since the advent of bridges. Polymer concretes have been in use as wearing surfaces on concrete decks for the past 25 years or so. Despite the advantages of polymer concrete, the most common materials used as wearing surfaces are hydraulic cement concrete and asphalt. However, in recent years, with the advent of FRP bridge decks, polymer concretes have become extremely popular because the advantages of such overlays do not counteract the advantages of FRP decks. Due to the relative unavailability of technical data (almost all work done with polymer concrete overlays has been trial and error) about polymer concrete overlays used on FRP bridge decks, an attempt is made herein to provide the reader with a background on polymer concrete overlays by summarizing their performance over the past 25 years and a past evaluation of PC overlays used with FRP bridge decks.

2.2 The Past 25 Years' Polymer Concrete Practice

Polymer concrete (PC) overlays have been used mainly on concrete bridge decks. PC overlays present many advantages over hydraulic cement and asphalt overlays. PC overlays add very little sustained load, have very fast cure times, only require typically 3/8 of an inch thickness, are essentially waterproof, are long lasting, and provide excellent skid resistance.

2.2.1 Overlay Materials

Polymer concretes have two primary components: the binder and the aggregate. Sprinkel (2001) states that the most commonly used binders are epoxy, urethane modified epoxy, polyester, and methacrylate. Polymer binders are usually two-component systems: one being resin and the other being a curing or initiating agent. There are several polymer binder systems available in the market for bridge deck wearing surface applications, for example, Tamms Flexolith® epoxy, Unitex Pro-Poxy III DOT® epoxy, Sikadur 22 Lo Mod® epoxy, Reichhold Polylite® isophthalic polyester, SRS Degadur® methacrylate, E-Bond 526, Poly Carb, Transpo

T-48, etc. Their properties are listed in Table 2.2.1.1 and their suppliers are appended in Appendix D. All these systems were originally formulated for bridge decks made of conventional materials such as Portland cement concrete and steel. The above epoxy-based systems meet ASTM C881: Standard Specification for Epoxy-Resin-Base Bonding Systems for Concrete (see Appendix C for ASTM test standards). The aggregates are usually specified to be dry (less than 0.2% moisture), angular-grained silica or basalt and free from dirt, clay, asphalt, and other organic materials (Sprinkel, 2001).

2.2.2 Construction Methods

The successful application of PC overlays depends on the following factors: 1) acceptable materials; 2) adequate surface preparation; 3) proper batching and placement of materials; and 4) adequate curing time before it is subjected to loading.

The most important step in construction of PC overlays is the surface preparation. Sprinkel (2001) specifies that for concrete decks the surface must be sound, clean, and dry. Sound concrete is specified as having a tensile strength of at least 150 psi and a chloride ion content at the reinforcing steel that is no greater than 1.3 lb/yd^3. Virginia Test Method 92 (VTM-92) specifies acceptable cleaning practices for concrete decks and test methods for the final overlay. There are no specifications, other than those of the manufacturer, for PC overlays when used on FRP decks. However, common sense tells us that the deck must be prepared by some method that leaves a fresh clean surface. Some common methods for achieving this with FRP decks are sanding and the use of a peel-ply on the outer layer of the deck surface, which is placed during the pultrusion process.

There are three primary methods of applying PC overlays. They are multiple layer broadcast application, slurry application, and premixed application. The overlay should be placed the same day as the surface preparation occurs (Sprinkel, 2001).

Typically, for the multiple layer broadcast method, a layer of binder is poured and the aggregate is broadcast to excess over the binder. After the initial set, the extra aggregate is removed and the same is repeated for the following layers until the desired thickness is achieved.

Table 2.2.1.1 The Characteristics of Some Polymer Concrete Overlay Binders

Binder Properties @75F	Test Method	ASTM C881 specifications	Tamms Flexolith	Unitex Pro-Poxy III DOT	Polycarb Flexogrid	Sikadur 22 Lo Mod	Transpo T-48	Reichhold Polylite	SRS Degadur	E Bond 526
Chemical type			Epoxy	Epoxy	Epoxy urethane	Epoxy	Polysulfide epoxy	Isophthalic polyester	Methacrylate	Epoxy
Color, Part A			Clear		Amber	Clear		Amber		Amber
Color, Part B			Amber		Amber	Light amber				
Mixing ratio by volume	Part A:Part B	None	1:1	1:1	2:1	1:1	2:1	100:1		1:1
Mixed viscosity @75F	ASTM D2393, Brookfield RVT	max 2000 cps	1700 cps	1425 cps		2500 cps	1200-1600 cps	700-900 cps	1100-1300 cps	1400-1850 cps
Density	ASTM D2849						1.05 gms/ml	1.14		
Gel time (100-200 gms)	ASTM C881, AASHTO T237	min 30 min	> 30 min @ 50F	30 min	22-31 min @75F	30 min	15-30 min @70F	5-7 min @150-190F	15-45	15-20 min
Peak exotherm								300-350F		
Gel time w. aggregate					1.5 hr@75F					
Initial cure	ASTM C109		3 hr		6 hr @75F			3hr	3hr	3hr
Final cure					48 hr- 7day					
Solids content	ASTM D1644		100%	100%	100%	100%	100%			
Ash content	ASTM D482		0.2%							
Volatile content			0.5%					29-32%		1.57%
Flash point	ASTM D1310						200F	89F		
Tensile strength	ASTM D638	None	2700 psi	2610 psi @7 days	>2500 psi	5900 psi	1800 psi	2000 psi	493-1204 psi	2900-3500psi
Tensile elongation	ASTM D638	min 30%	45%	49% @7days	35+-5 %	30% @0.5in/min	45%	50%	100-200%	40-70%
Tensile modulus	ASTM D638		90-130 kpsi			190 ksi				
Flexural strength	ASTM D790					6800 psi		yields		
Flexural modulus	ASTM D790					277 ksi		yields		
Shear strength	ASTM D732					5400 psi				

Table 2.2.1.1 The Characteristics of Some Polymer Concrete Overlay Binders (cont'd)

Binder Properties @75F	Test Method	ASTM C881 specifications	Tamms Flexolith	Unitex Pro-Poxy III DOT	Polycarb Flexogrid	Sikadur 22 Lo Mod	Transpo T-48	Reichhold Polylite	SRS Degadur	E Bond 526
Compressive strength	ASTM D695		5000 psi		7-9 kpsi @ ASTM C109	8200 psi @14days	5000 psi			
Compressive modulus	ASTM D695	max 130 kpsi	90-130 kpsi	64,820 psi		150 ksi				
Bond strength	ASTM C882	min 1500 psi	1800 psi	3470 psi @14 days		1600 psi @ moist cure				1950 psi @7 day dry
Hardness, Shore D	ASTM D2240	None	65	69	65+-5		60	74		
Water absorption, 24hr	ASTM D570	max 1%	< 0.5%	0.19%	0.2%	0.232%				0.40%
Abrasion resistance -Wear index, 1000 cycle	ASTM C501				75-85 mg /1000 gms, CS-17 wheel	1.61gm /1000gm 1:2.25 Mortar, H-22 wheel				
Flexural creep at low temp, total movement	California Test 419				0.0065 in in 7 days, min					
Thermal compatibility (no delamination of overlay)	ASTM C884	None	Pass	Pass						Pass
Effective shrinkage	ASTM C883	Pass	Pass	Pass						Pass
Chloride permeability	AASHTO T277, ASTM C1202	None	<100 coulombs	0.9 coulombs						73 Coulombs
Acid number								11		
Mortar Properties			1:3 parts sand	1:3.5 parts sand		1: 2.25 parts sand				1:3.25 parts loose agregate
Tensile strength	ASTM D638					2200 psi	1800 psi @ASTM C307			
Tensile modulus	ASTM D638					478 ksi	600 kpsi			
Elongation at break	ASTM D638					1.1%				

Table 2.2.1.1 The Characteristics of Some Polymer Concrete Overlay Binders (cont'd)

Mortar Properties	Test Method	ASTM C881 specifications	Tamms Flexolith	Unitex Pro-Poxy III DOT	Polycarb Flexogrid	Sikadur 22 Lo Mod	Transpo T-48	Reichhold Polylite	SRS Degadur	E Bond 526
Compressive strength	ASTM C109	5000psi@24hr ;1000psi@3hr ASTM C579	7000 psi @24hr 75F 1400 psi @4hr 75F	7500 psi @24 hr; 1100 psi @ 3hr ASTM C579		3150 psi @24 hr; 6900 psi @ 3days ASTM D695	5000-7000 psi			6800 psi @46 hr; 1300 psi @ 3hr ASTM C579
Compressive modulus	ASTM C109		90-140 kpsi			125 ksi @7days				340ksi@7days
Flexural strength	ASTM D790		2000 psi			4300 psi	1800 psi			
Flexural modulus	ASTM D790		225 kpsi			906 ksi	440 kpsi			
Shear strength	ASTM D732					3300 psi @1:5 Mortar				
Adhesive strength to concrete	ACI 503R-30 ASTM D4541 VTM92	>250 psi	250 psi concrete failure	250 psi @24 hr	Concrete failure		>250 psi substrate failure			310 psi
Deflection temp	ASTM D648					111F @1:5 Mortar				
Permeability (electrical resistance)	High input impedance ohmmeter		500,000 ohms							
Coefficient of thermal expansion	ASTM C531						20-24E-6 in/in /F			
Freeze-thaw resistance	ASTM C666						Pass (no change)			
Wet skid resistance	ASTM E274		45-60		> 50		50			
Product note			low mod, low temp, two comp, moisture insensi, rapid cure, ASTM C881 for concrete, >25yr service	low mod, low viscosity, solvent-free, two comp, moisture insensi, ASTM C881	Mark-163 co-polymer system for concrete, metal, asphalt, two comp	low mod, medium viscosity, solvent-free, two comp, moisture insensi, ASTM C881	low mod, durable, cost effective, two comp. for concrete and FRP decks	flexible, low reactivity, low viscosity, low shrink Polylite 31830 (prepromoted version 32300)	solvent free, VOC compliant, 100% reactive, no technical data available	low mod, flexible, 100% solids, two component, moisture insensitive, waterproofing, rapid cure

For the slurry application method, a primer is spread over the area and the PC slurry is then applied. Then, more aggregate is then broadcast over the surface and then removed after the initial set. A sealer may or may not be used for this method.

With the premixed method, a primer is typically used and then the PC is spread over the area. A vibratory screed is then used to consolidate and strike off the PC. Continuous batching and paving equipment has also been used with this method (Sprinkel, 2001). Grooves or broadcast aggregate may be needed with this method in order to obtain adequate skid resistance.

2.2.3 Performance

Performance of PC overlays on concrete bridge decks is typically judged in terms of tensile bond strength, chloride ion permeability, skid resistance, and service life. According to Sprinkel (2001), most typically used PC overlays perform as good as or better than hydraulic cement overlays and have an expected service life of 25 years.

2.2.4 Cost

Cost is one of the largest issues in the construction industry. When compared with hydraulic cement concrete overlays, PC overlays are typically 25% less based on total initial cost and 36% less based on life cycle cost (Sprinkel 2001). The cost savings occur because of the following reasons: 1) less time required for application; 2) less requirements for traffic rerouting ie. repainting lines, barriers, etc. 3) no need for raising approach slabs, joints, backwalls, etc.

2.3 Past Evaluations

The construction of two bridges in West Virginia in 1997 utilizing FRP decks brought rise to the need for the evaluation of a suitable wearing surface, although there was a research report entitled “Wearing Surface Testing of Modular Fiberglass Bridge Deck System” by Deshpande (1992) who presented a feasibility study of polyester and epoxy resins used as wearing surface for the fiberglass bridge deck system. Herein, discussion is mainly based on the work by researchers at CFC-WVU, where a thin PC overlay made with isophthalic unsaturated

polyester resin and fine silica sand was used (Lopez-Anido, et al., 1998; Vendam, 1997). This overlay was used in two FRP bridges – Laurel Lick bridge and Wickwire Run bridge- and was proved of satisfactory performance (Ray Publishing, 1997; Justice, 2004).

2.3.1 Material Description

For this evaluation the PC overlay was applied to a portion of the FRP deck, simulating field placement, and seven specimens with PC overlay bonded to the FRP were then cut from the deck. Separate FRP and PC specimens were also tested to establish individual properties.

The evaluation use half-depth trapezoidal sections connected by means of full-depth hexagons. The fabric architecture was in the form of multi-axial stitched fabrics, continuous rovings, chopped strand mats, and continuous fiber mats, all made of E-glass fibers. Vinyl Ester resin was used as the matrix for the deck. The deck was manufactured by Creative Pultrusions, Inc. under the trade name of Superdeck^{TM} (Lopez-Anido, 1998).

Reichhold's Polylite® 32300 isophthalic unsaturated polyester (UPE) resin was used, along with methyl ethyl keytone peroxide as a curing agent, for this evaluation. This resin is flexible, has a low reactivity, and is pre-promoted for room temperature cure (Lopez-Anido, 1998). Atprime®-2 was used as a primer. The PC overlay was then applied using the broom and seed method with a resin-to-aggregate ratio of 1 to 3.

2.3.2 Experimental Program

2.3.2.1 Coupon Testing

Standard bending and tension test were conducted of the FRP coupons the extensional elastic modulus and the bending elastic modulus. These results were then correlated with analytical computations based on mechanics of laminated beams (Lopez-Anido, 1998). The elastic bending modulus of the PC coupons were determined using a three-point bending test.

2.3.2.2 Beam Testing

A three-point bending test with a load rate of 250 lb/min. was used for the beam specimens. The specimen tested with the PC in tension failed primarily in the PC for strain

levels higher than 2%, with a secondary failure though either interlaminar shear failure in the FRP or tension failure in the FRP. The specimens with the PC overlay in compression failed in the FRP substrate. No debonding was observed between the PC overlay and the FRP (Lopez-Anido, 1998).

2.3.3 Evaluation of Data

The location of the neutral axis and the bending stiffness of the FRP-PC beam specimens in the linear range were computed analytically and are expressed by equations (1) and (2) (Lopez-Anido, 1998).

$$y_n = \frac{E_x^o t \frac{t}{2} + E_{PC} t_{PC}\left(t + \frac{t_{PC}}{2}\right)}{E_x^o t + E_{PC} t_{PC}} \tag{1}$$

$$EI = \left[\frac{E_x^f t^3}{12} + E_x^o t\left(y_n - \frac{t}{2}\right)^2 + \frac{E_{PC} t_{PC}^3}{12} + E_{PC} t_{PC}\left(\frac{t_{PC}}{2} + t - y_n\right)^2\right] \cdot b \tag{2}$$

It was found that the contribution of the PC to the bending stiffness was only 10% and thus was neglected for design purposes (Lopez-Anido, 1998). An analytical model based on Eqns. (1) and (2) was used to compute the design limit load and it was found that increasing the thickness of the overlay from 3/8-in. to ¾-in resulted in a 15% reduction of the design load (Lopez-Anido, 1998).

2.3.4 Field Placement

The first field placement was done at the Laurel Lick Bridge. The PC overlay was applied by a crew from the West Virginia Division of Highways. First the surface was prepared by sandblasting. Then, the polyurethane primer was applied and allowed to moisture cure. The PC overlay was then applied using the broom and seed method to a thickness of 3/8-inch. A similar method was used for the Wickwire Run Bridge except a thickness of ½-inch was used. For large decks a more mechanized method of placement or placement at the factory is needed (Lopez-Anido, 1998).

2.3.5 Review

The FRP-PC beam specimens exhibited high tensile elongation and excellent adhesion. The UPE resin binder in combination with the FRP surface treatment was successful. The ultimate tensile elongation of the PC overlay exceeded 2% (Lopez-Anido, 1998).

2.4 Conclusion

This chapter gives a brief overview of how PC overlays have been used in the past 25 years, some problems associated with their use on FRP decks, and a brief look at some past evaluations of PC overlays used on FRP bridge decks.. The information in this chapter has been presented in order to better define the goals of this report and give the reader a better understanding of PC overlays and why this work is necessary.

3. COEFFICIENT OF THERMAL EXPANSION TESTING

3.1 Introduction

Each polymer has a different thermal response when subjected to a temperature change, and a lack of compatibility in thermal properties between the FRP deck and the polymer concrete wearing surface can lead to debonding and/or cracking of the wearing surface. Therefore, characterization of coefficient of thermal expansion for the principal materials involved is a very important step toward understanding the existing problems and improving the long-term performance of the wearing surfaces.

The coefficient of thermal expansion (CTE) of a material is generally defined as the fractional increase in length per degree increase in temperature. The exact definition varies, depending on whether it is specified at a precise temperature (true coefficient of thermal expansion) or over a temperature range (mean coefficient of thermal expansion). Here, the coefficient of linear thermal expansion over a temperature range of 75°F-180°F was determined for the three resin binders and their respective polymer concretes.

3.2 Specimen Preparation

Both neat resin and polymer concrete sheet samples were cast following application guidelines provided by the resin binder suppliers (see for example, E-Bond 526 User Guide, 2000) or DOT's Guidelines (for example, VDOT Guideline, 1993). For polymer concretes, sand aggregates were mixed with resin binder at a ratio of 1:2 by volume in a container. Then testing specimens measuring ½ x 2 x ¼ inches were cut from the fully cured neat resin and polymer concrete sheet samples (Figure 3.2.1). Three resin binders in neat resin and polymer concrete plus three replications gives a total of 18 testing specimens.

3.3 Test Method

The CTE measurements were accomplished using the environmental chamber of the Instrom machine. A strain gage was bonded onto the representative surface area of the sample, as

shown in Figure 3.2.1. One end of the sample was mounted on the grips inside the environmental chamber. The other end was pending in the space so that the test section area of the sample was subjected to uniform thermal expansion in a free space as the specimen gets heated. The degree of the expansion was monitored from the readings of a strain gage indicator. The self expansion of the strain gauge could be identified by subjecting a as-received strain gauge to the same temperature profile and then subtracted from the readings of the strain gauge on the sample. The coefficient of thermal expansion was calculated from the slope of the curve obtained by plotting the strain readings versus the temperature. This method was verified by testing a known material with a known value of coefficient of thermal expansion (Liang et al, 2001).

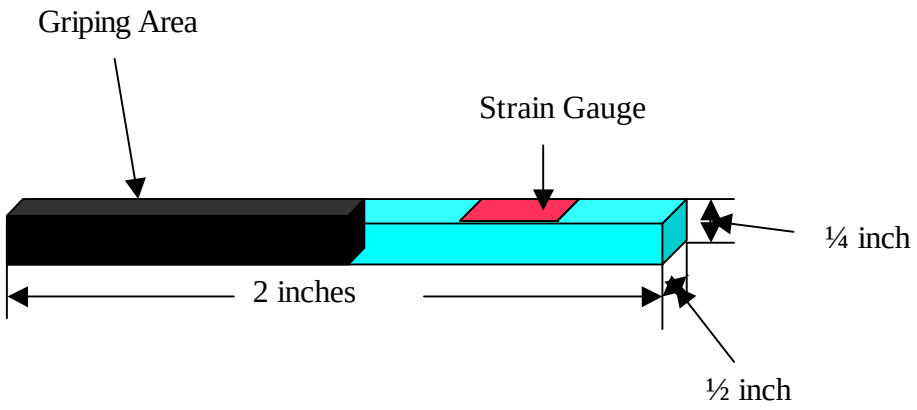

Figure 3.3.1: Specimen schematic for CTE measurement.

In this study, the test temperature ranged from 75^0F to 180^0F. The temperature chamber was allowed to stabilize at a particular temperature for a short period (about 5 seconds) and then the readings of the strain indicator were noted. Note these resin binders are flexible elastomers. It was observed that for neat resin binder samples, the specimen would significantly creep under its self-weight at high temperatures if the equilibrium (stabilization) time were set longer. Placing the sample horizontally on a flat surface was considered but was not used after noticing the friction between the sample and surface would affect the expansion of the sample. The compact size and efficient heat convection features of the environmental chamber made it possible to reach the set temperature within one to two minutes. The measurements were limited

to 180^0F in order to avoid possible bonding failure of the strain gage at higher temperatures. It takes approximately half an hour to conduct each test.

3.4 Results

The microstrain data as a function of temperature for three resin binders and the prepared polymer concretes are plotted in Figures 3.4.1 –3.4.6 respectively. The slope of each set of data, that is, the coefficient of thermal expansion of the corresponding material, was calculated through linear fitting. Raw experimental data were appended in Appendix B. As seen from the plots, the polymer concrete samples yield more consistent CTE values.

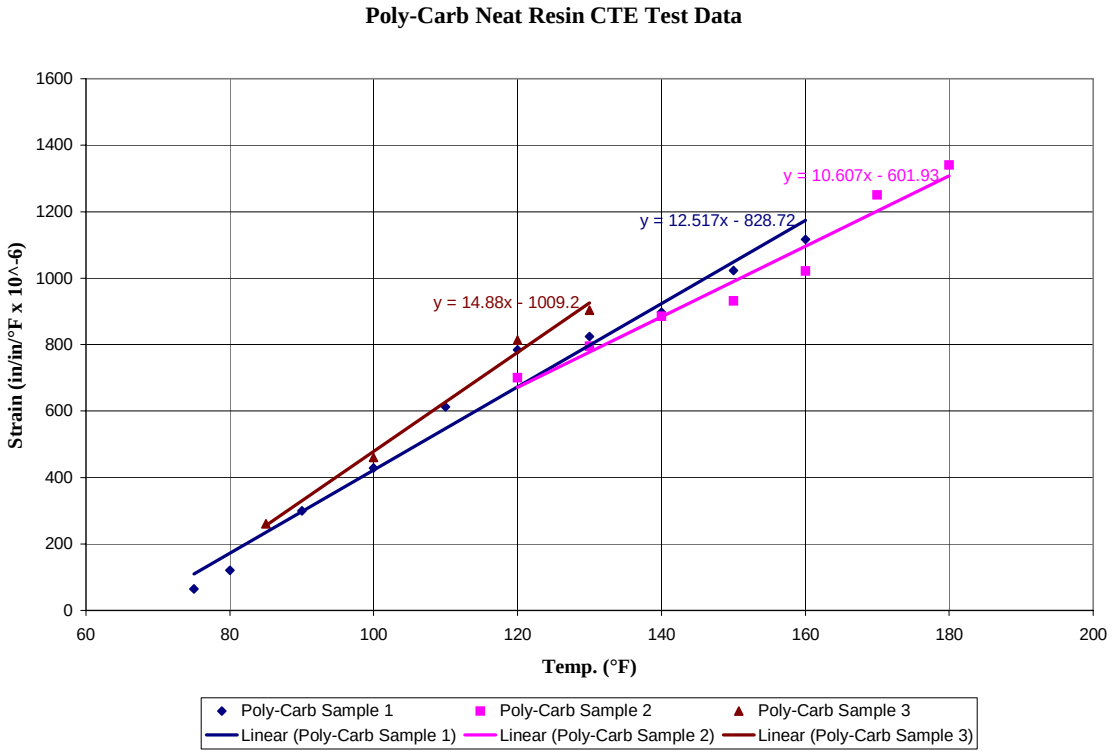

Figure 3.4.1: The thermal expansion (microstrain) versus temperature data for Polycarb Mark-163 resin binder.

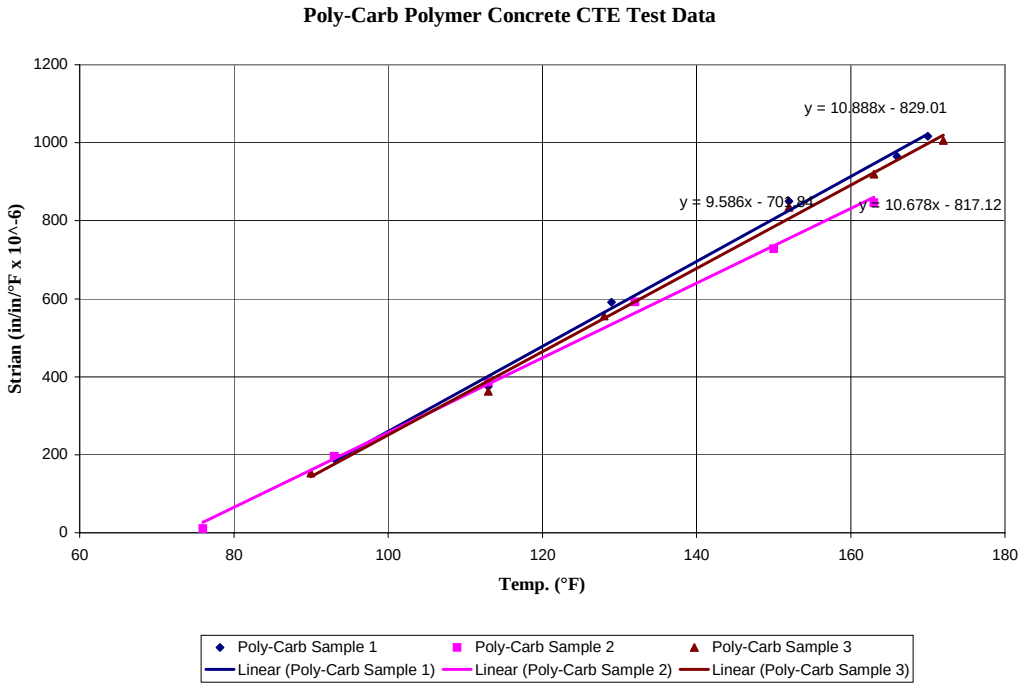

Figure 3.4.2: The thermal expansion (microstrain) versus temperature data for Polycarb Mark-163 polymer concrete.

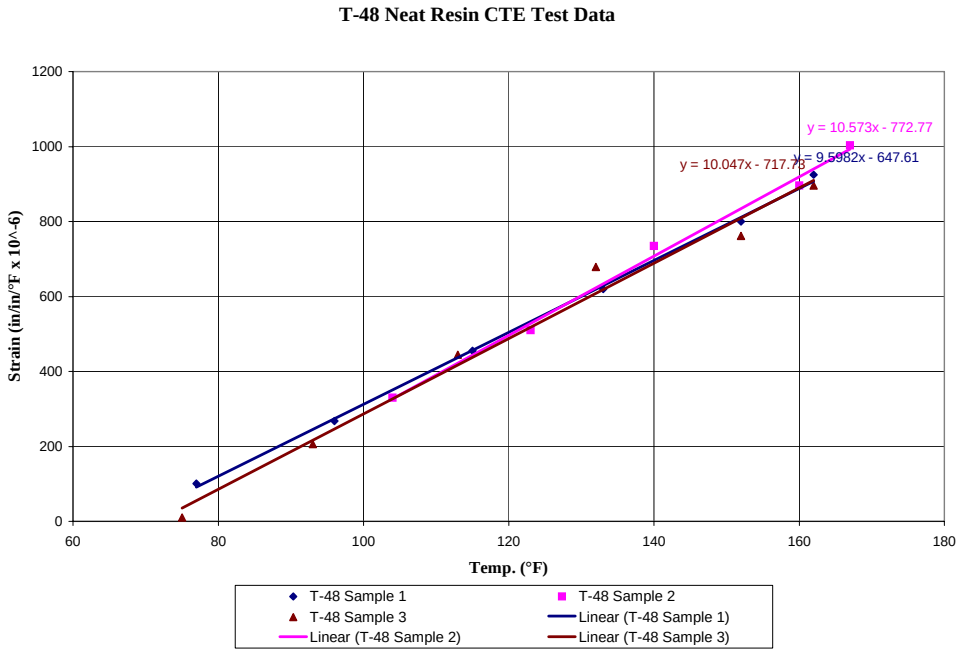

Figure 3.4.3: The thermal expansion (microstrain) versus temperature data for Transpo T-48 resin binder.

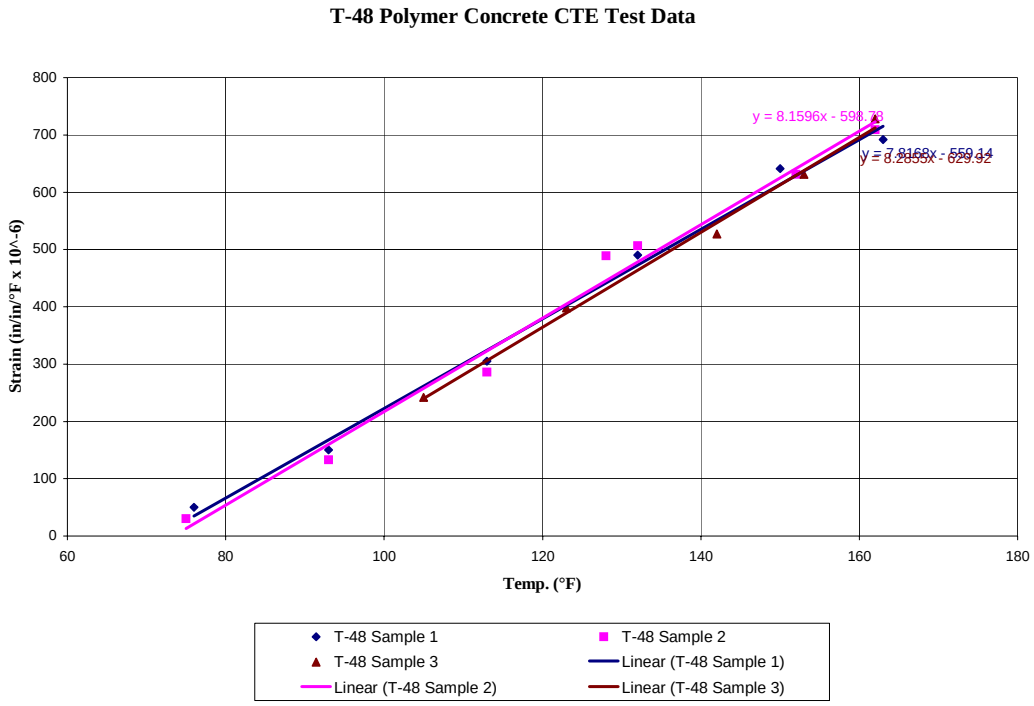

Figure 3.4.4: The thermal expansion (microstrain) versus temperature data for Transpo T-48 polymer concrete.

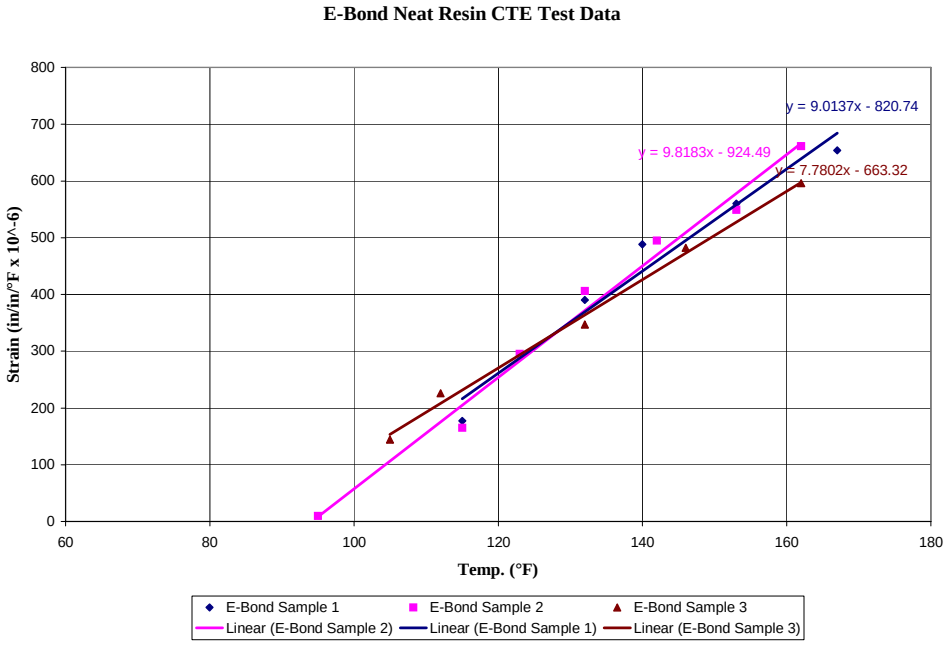

Figure 3.4.5: The thermal expansion (microstrain) versus temperature data for E-Bond 526 resin binder.

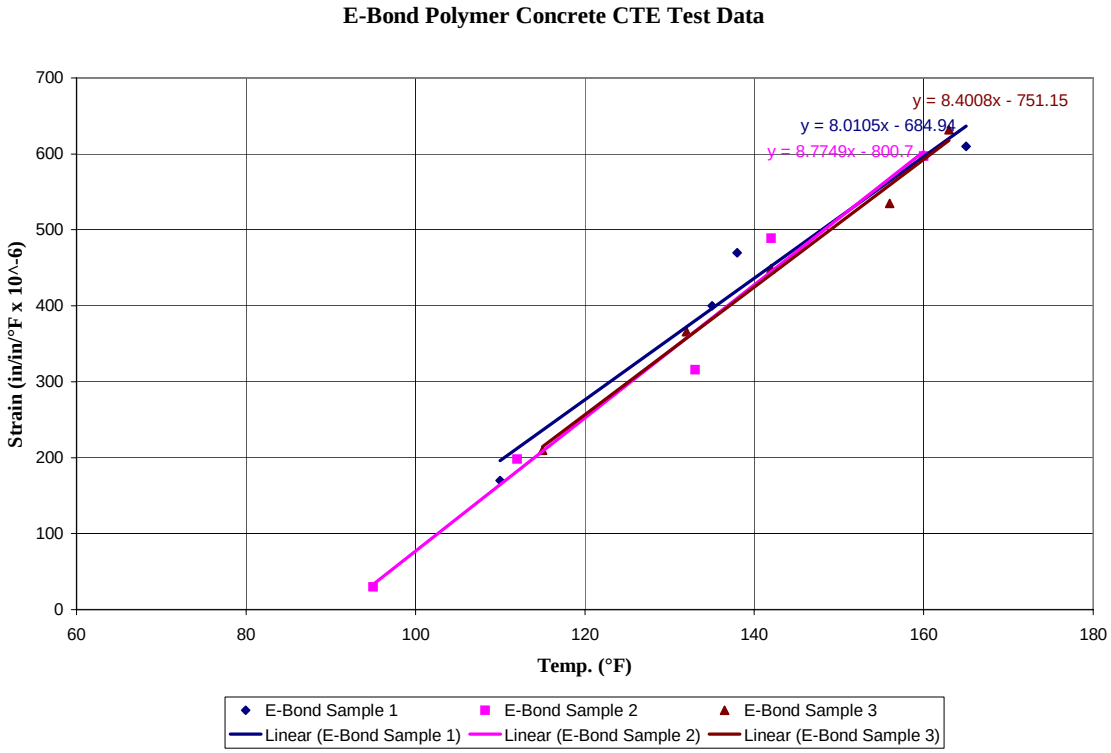

Figure 3.4.6: The thermal expansion (microstrain) versus temperature data for E-bond 526 polymer concrete.

3.5 Discussion & Conclusions

The results illustrated in Figures 3.4.1 to 3.4.6 can be summarized in Table 3.5.1. The following points can be drawn from the CTE testing: 1) For a given polymer binder, the polymer concrete has a lower coefficient of thermal expansion than the neat resin because of the presence of sand aggregates. As seen in Table 3.5.1, for all three resin binders, the standard deviation is much smaller in the case of polymer concrete than that of neat resin. This is consistent with the trend of those linear fits as discussed earlier; 2) E-Bond 526 neat resin shows a lowest coefficient of thermal expansion, implying a better compatibility with that of FRP (3.3-5.6 E-6 in/in/°F) than Polycarb Mark-163 or Transpo T-48. However, T-48 Polymer concrete has the lowest CTE value, implying that T-48 PC has the best compatibility with FRP. Note that the T-48 polymer concrete, instead of E-Bond 526 polymer concrete, has the lowest standard deviation. This might be due to, we believe, the variation of content of sand aggregates and /or improper location

of the strain gage. In addition, our measurements yielded a CTE value of 10.07 E-6 in/in/°F for Transpo T-48 neat resin, much smaller than 20-24 E-6 in/in/°F as shown in the technical data sheet of the supplier (Table 2.1). Some possible reasons may include different specimen dimensions, different test methods, and not sufficient equilibrium time before taking strain gage readings at each set temperature.

In conclusion, both Transpo T-48 and E-Bond 526 have a better thermal compatibility with FRP than Poly Carb Mark-163.

Table 3.5.1: Coefficients of thermal expansion of polymer binders and concretes investigated

	Neat Resin 10E-6 in/in/F	Polymer Concrete 10E-6 in/in/F
Polycarb Mark-163	12.67 $\pm$ 2.14	10.38 $\pm$ 0.7
Transpo T-48	10.07 $\pm$ 0.49	8.09 $\pm$ 0.24
E-Bond 526	8.87 $\pm$ 1.03	8.40 $\pm$ 0.38

4. DEVELOPMENT OF STRAIN VARIATION DIAGRAM

4.1 Introduction

Strain variation diagram is a plot of strain versus specimen thickness describing how the strain develops and transfers throughout the specimen. The strain variation diagram is used mostly in the flexure mode design. In this study, the strain variation diagram is used as a way of revealing the compatibility between the polymer concrete and FRP deck materials. An incompatible combination would lead to potential delamination of the polymer concrete wearing surface. Different materials have different moduli of elasticity, intrinsically leading to a strain discontinuity at the interface between two different materials, such as FRP and polymer concrete. One can assume that the lesser the strain shift at the interface the more compatible the binder is with the FRP. By measuring and comparing the strain variation diagram for each resin binder, we can conclude which of the polymer binders is most compatible with FRP. This chapter presents the strain variation diagrams for FRP deck plates with polymer concrete overlays made of those three representative commercial resin binders, i.e. Polycarb Flexogrid Mark-163, E-Bond 526, and Transpo T-48.

4.2 Specimen Preparation

The specimens used for strain variation diagram measurements were coupons of dimensions ½ x 5 ½ x ½ inch cut from FRP deck plates, and were coated with a 3/8 inch layer of polymer concrete on top (see Figure 4.2.1). As illustrated in Figure 4.2.1, three strain gauges were mounted on each specimen, one placed on the top and one at the bottom of the specimen, and one placed at the interface between the polymer concrete and the FRP composite. The embedment of a 4^{th} strain gauge in the middle of the polymer concrete layer was attempted and found to be too difficult to accurately place this gauge at such a thin layer of polymer concrete. One strain gauge was successfully mounted in the middle but this strain gauge failed quickly during testing.

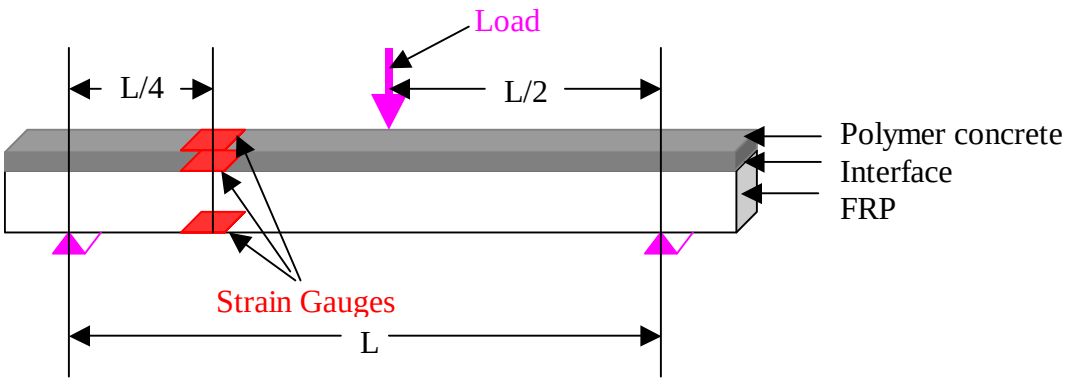

Figure 4.2.1: Specimen schematic for strain variation diagram measurement

4.3 Test Method

The three point bending test was used to determine the strain variation along the specimen thickness. Tests were conducted in a batch mode at different loads ranging from 50 lbs to 400 lbs, with the maximum being about half of the specimen failure load ~ 800 lbs. The strain data was collected from three strain gages mounted at different positions across the specimen thickness direction (Figure 4.2.1). The strain across the FRP coupon thickness can be assumed as linear and under this test, it is assumed that the strain variation is linear in the polymer concrete as well. This assumption is thought to be valid because of the relatively thin layer of the polymer concrete (3/8 in).

Since the strain gauge that should be placed in the middle of the polymer concrete layer was abandoned due to difficulty of correct placement, the strain near the interface for the polymer concrete had to be calculated analytically. This was accomplished by equating internal moment with the externally applied moment. The analysis began by using $\sigma = E\varepsilon$ to obtain the stresses and then using $f = \sigma * A$ to obtain force where σ is stress, E is modulus of elasticity, e is strain, f is force, and A is area. The internal moment resisted by the polymer concrete is then calculated by adding the moment created by the tension and compression forces in the FRP, then subtracting it from the external moment created by the load. Finally, the obtained moment resisted by the polymer concrete is used to find the missing strain point for the polymer concrete.

4.4 Results

Two sets of specimens for three types of resin binders plus two runs for each specimen make total 12 tests. Consistent results were obtained for three resin binders. Representative strain variation diagrams for Polycarb Mark-163, Transpo T-48, and E-Bond 526 are shown in Figures 4.4.1 to 4.4.3, respectively. Raw experimental data were appended in Appendix B.

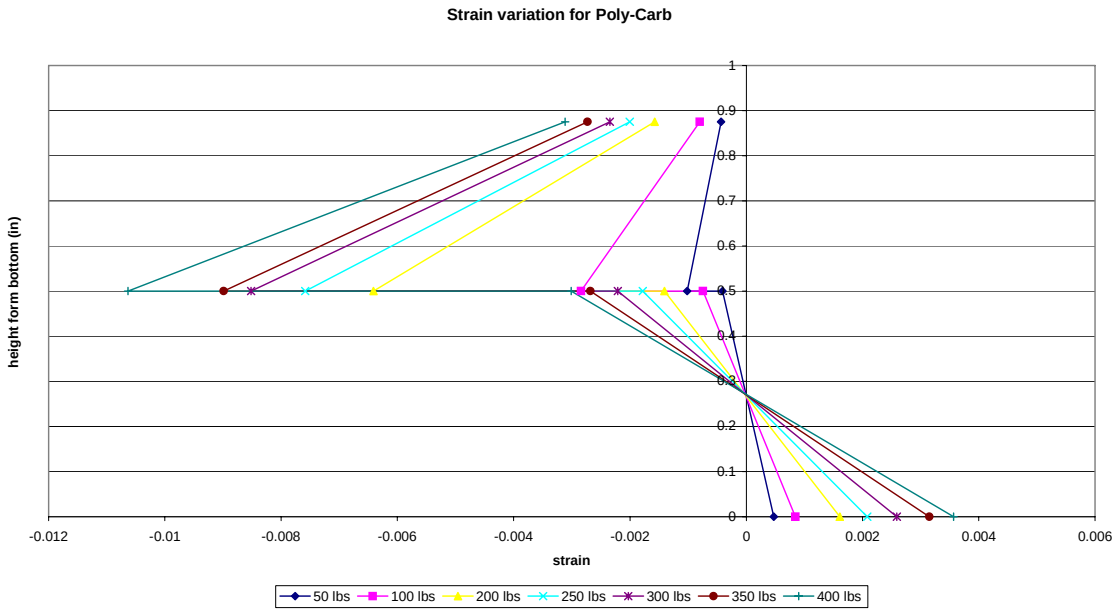

Figure 4.4.1: Strain variation diagram for Polycarb Mark-163

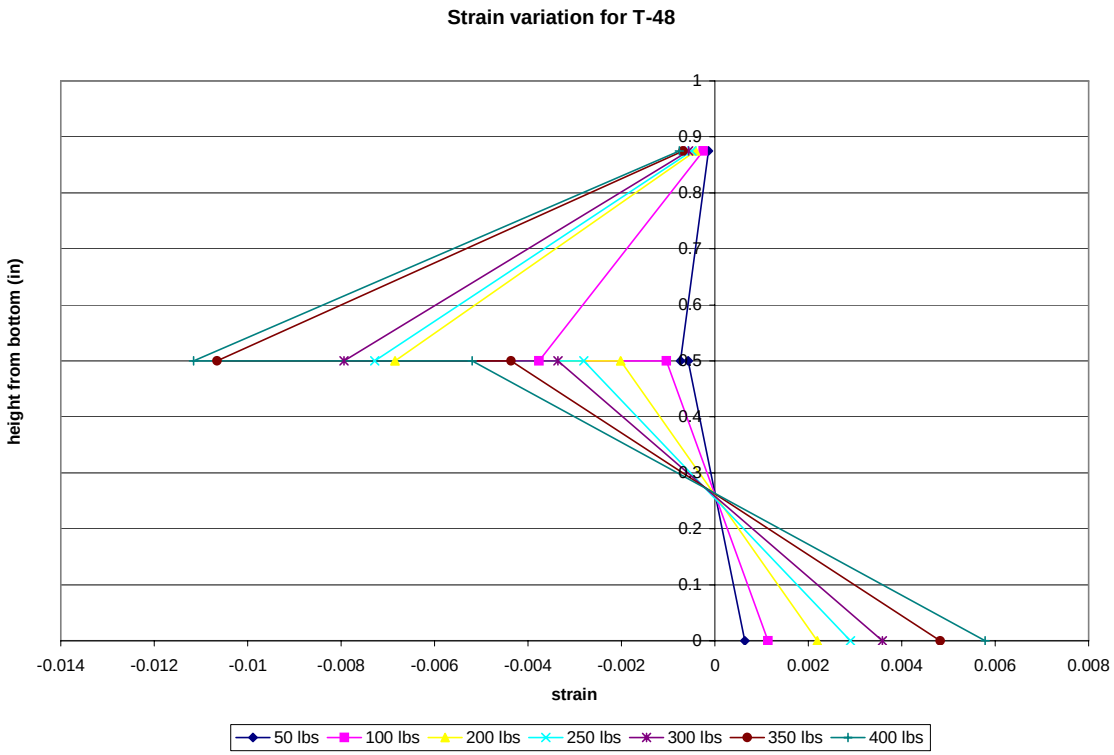

Figure 4.4.2: Strain variation diagram for Transpo T-48

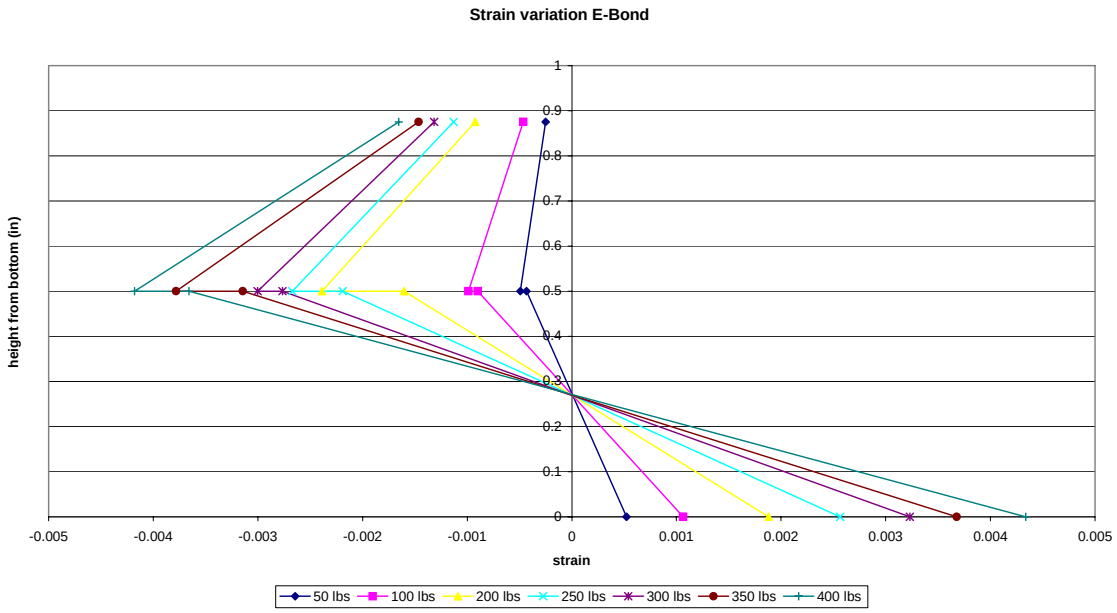

Figure 4.4.3: Strain variation diagram for E-Bond 526

In the graphs, strain data (x-axis) obtained under various loads is plotted as a function of height from bottom (y-axis) across the thickness direction. The lower 1/2 inch represents FRP deck while upper 3/8 inch represents polymer concrete. Positive strain data represents tension strains while negative strain data represents compression strains. All the data shown were obtained when the polymer concrete was loaded on the top and subjected to compression. Please note that there were two sets of strain data at the interface between the polymer concrete and the FRP. The strain data for the FRP were experimentally collected from strain gauge readings but the strain data for polymer concrete were analytically calculated in the method described earlier.

4.5 Discussion & Conclusions

The results illustrated in Figures 4.4.1 to 4.4.3 indicate the following points: 1) Microstrain development patterns in the FRP decks with increasing the load are nearly the same, independent of overlay systems; 2) Strain discontinuity at the interface between FRP and the polymer concrete occurs more or less for all three overlay systems; 3) E-Bond 526 overlay system shows smaller difference in interface strain between FRP and the polymer concrete, which denotes a better compatibility between the two materials; and 4) Polycarb Mark-163 and Transpo T-48 have relatively larger difference in interface strain between FRP and the polymer concrete, and these two resin binders have similar strain variation diagrams.

These observations are well in agreement with the properties of the polymer resin binders. All three resin binders have larger elongation to failure. But E-Bond 526 has highest modulus of elasticity, consistent with the smallest strain at a given load while T-48 and Mark – 163 have lower modulus of elasticity, leading to larger strain at a given load.

Therefore it can be concluded from the results presented above that the polymer concrete made of E- Bond 526 has better strain compatibility with FRP deck panels than those made of Transpo T-48 and Polycarb Mark-163, while the polymer concretes made of Polycarb Mark–163 and Transpo T-48 over FRP decks have similar strain compatibility. It implies that E-Bond 526 would produce a polymer concrete overlay on FRP bridge decks that is least likely to crack, de-bond, or delaminate due to a mismatch of stiffness properties.

FRP composite has a much larger modulus of elasticity than that of the polymer concretes tested. At a given load, polymer concrete should yield a much larger strain deformation than that of FRP. However, it is observed from the strain variation diagrams reported above that for all three types of overlay systems the strain on the polymer concrete surface is unexpectedly small as compared to the calculated strain at the interface. At the beginning, it was suspected that the correctness of strain gauge placement: a poorly placed strain gauge on the polymer concrete would certainly under-estimate the actual deformation. Repeat tests were conducted and similar results were obtained.

Such phenomena may be attributed to the energy absorption ability of the polymer concrete, prestressing effects offered by FRP onto the thin polymer concrete wearing surface due to FRP's higher modulus (thicker polymer concrete than 3/8 inch may alter the current observation), and a strain slippage at the interface between polymer concrete and FRP. This stain slippage validates the assumption of linear strain in the Polymer concrete.

The polymer concrete has relatively higher percentage of elongation, which denotes a higher energy absorption capability. Since the moment being resisted by the polymer concrete is relatively negligible compared to that of the FRP, the polymer concrete, due to the strain slippage at the interface, apparently absorbs the energy. This phenomenon was confirmed by testing each type of sample twice with the polymer concrete in tension instead of compression. The strain variation diagrams of these tests were basically identical to those of the polymer concretes being in compression except the negative strain values becoming positive strain values. Drawing a strait line on the side of the sample and subjecting it to bending load also confirmed the strain slippage, because the line did not remain straight. Such an energy absorption characteristic of polymer concrete would yield surface crack resistance.

If the above discussions are correct, both strain compatibility with FRP deck and energy absorption/strain slippage characteristic of polymer concrete shall be equally considered. Among the three resin binders investigated, their strain compatibility with FRP follows the following order: best E-Bond 526 > better Transpo T-48 > good Polycarb Mark-163 while their energy absorption ability follows in the following order: best Transpo T-48 > better Polycarb Mark-163 > good B-Bond 526.

5. BOND STRENGTH TESTING

5.1 Introduction

One of the current problems with wearing surfaces is that they are debonding from the FRP surface. Therefore, a resin binder with the best mix of bond strength, ductility, and durability is desired. Bond strength is the strength with which the polymer binder adheres to the surface. Several factors may contribute to failure in bond strength, including: 1) chemical properties of the binder and surface, 2) mismatching of thermo-mechanical properties (i.e. coefficient of thermal expansion, etc.), 3) presence of contaminants (i.e. dirt, oil, etc.), and 4) improper surface preparation. The effects of thermo-mechanical properties were discussed in Chapters 3 & 4. This Chapter will discuss the effect of surface preparation. The goal of the study is to determine the optimal surface preparation by establishing the relationship between bond strength and the level of surface preparation, and the most practical method of surface preparation by comparing the sanding method with a commercial peel-ply system. The bond strength data at different surface preparation levels are presented in comparison with the results from peel-ply surfaces for three representative commercial resin binders.

5.2 Specimen Preparation

In addition to three selected commercial resin binders, the materials used included two types of FRP deck plates. One type of deck plates were pultruded without peel-ply on the surface while the other with peel-ply on the surface. Both types were provided by Bedford Reinforced Plastics Inc.

12 inches long by 5-½ inches wide by ½ inch thick FRP plates were used for the test, and each plate was divided into four sections (see Figure 5.2.1 for reference). A ¼ inch section of 1-¼ inch diameter PVC pipe was used to control the area of binder used in the test. The surface of the FRP plate was sanded using different grit sand papers, with one quarter of the plate being left unsanded for use as a reference, and the other three being sanded with 180 grit (a fine preparation), 100 grit (a medium preparation), or 60 grit (a rough preparation) sandpaper erespectively. The PVC pieces were then placed on the FRP surface and the binders were poured into the PVC pieces with the smoothest surface possible. Once the binder cured, the

adhesive Pliogrip was used to bond a steel plate, with an arm welded to it to allow for the Instron machine to grip the plate, to the surface of the binder, as shown in Figure 5.2.1.

Use of PVC pipe sections was found critical to yield reliable and reproducible results. The function of using PVC pipe sections is to well control the accurate bonding area and thus effectively eliminate the boundary effect. Such a satisfactory bond strength test method awas arrived at after several improvements. Before using a thin section of PVC pipe to hold the resin and prevent any leakage, during preparation of the specimens, some of the resin binder would leak under the aluminum foil separator that was used for control of an accurate bond area. Those extra resins/bonds around the bonding area added the boundary effect, contributing to the overall bond strength and contaminating the data. All PVC pieces were left in place because removing them presented some margin for possible damage to the specimens, and none of the polymer binders bond to the PVC.

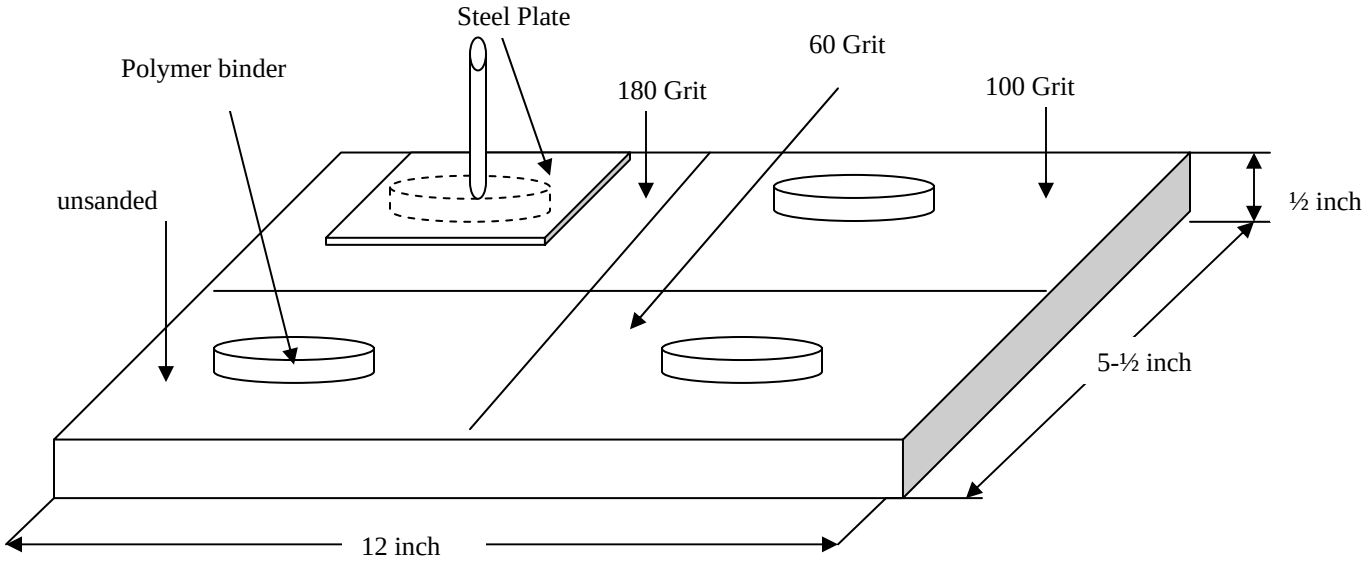

Figure 5.2.1: Specimen preparation and dimensions

Samples were also made in the same manner as above using FRP plates with a medium roughness peel-ply, instead of sanding for the surface preparation. A peel-ply is a permeable cloth layer added to the surface of the FRP plate during manufacturing that can then be peeled off during construction to reveal a fresh, clean, and textured surface ready for polymer concrete

application. These samples were 12 inch by 4 inch by ¼ inch. No preparation is required with the peel-ply method.

5.3 Test Method

The test was conducted on the Instrom machine. The lower loading arm is fitted with a flat compression plate and the upper arm is fitted with tension grips. The specimen is then clamped to the compression plate while the gripping arm of the specimen is clamped securely by the tension grip, as shown in Figure 5.3.1. The test was carried out in a position control mode at a rate of 0.3 inch per min until failure of specimen. The failure load in each test was recorded by Instron load cell. The failed sample was inspected for its failure mode (failure in FRP, failure in polymer concrete, or failure at the interface). Three sets of specimens for each resin binder, each set consisting of four surface roughness levels, were tested. From the failure load, bond strength can be calculated. This test method is essentially the same as VTM –92 (1993).

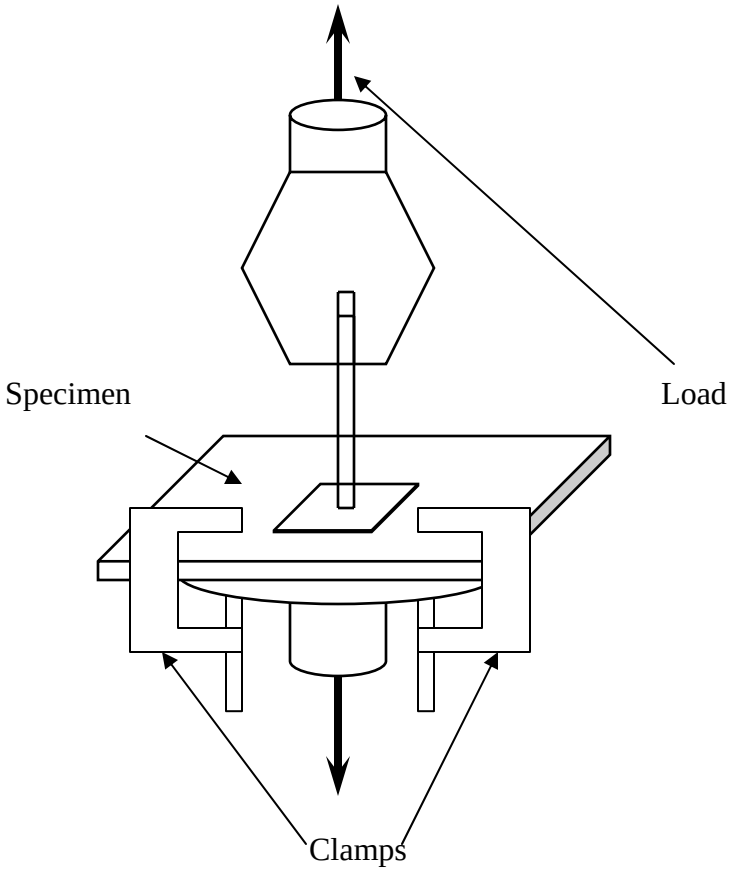

Figure 5.3.1: Schematic of bond strength test setup

5.4 Results

The results are presented as a bond stress in pounds per square inch at each surface preparation level. The bond stress is obtained by the equation $\sigma = F/A$, where F is the measured load in pounds and A is the area of a 1-¼ inch diameter circle. The grit starts with the least preparation, which is no surface preparation, and goes up in surface roughness. Figure 5.4.1 reports the average of two sets of test data for each sanding level. Figure 5.4.2 reports the data from three tests per binder for the peel-ply method. Please note that in Figure 5.4.2, each datum point represents one single test result, i.e. average of three points giving representative value for each binder. Raw experimental data were appended in Appendix B.

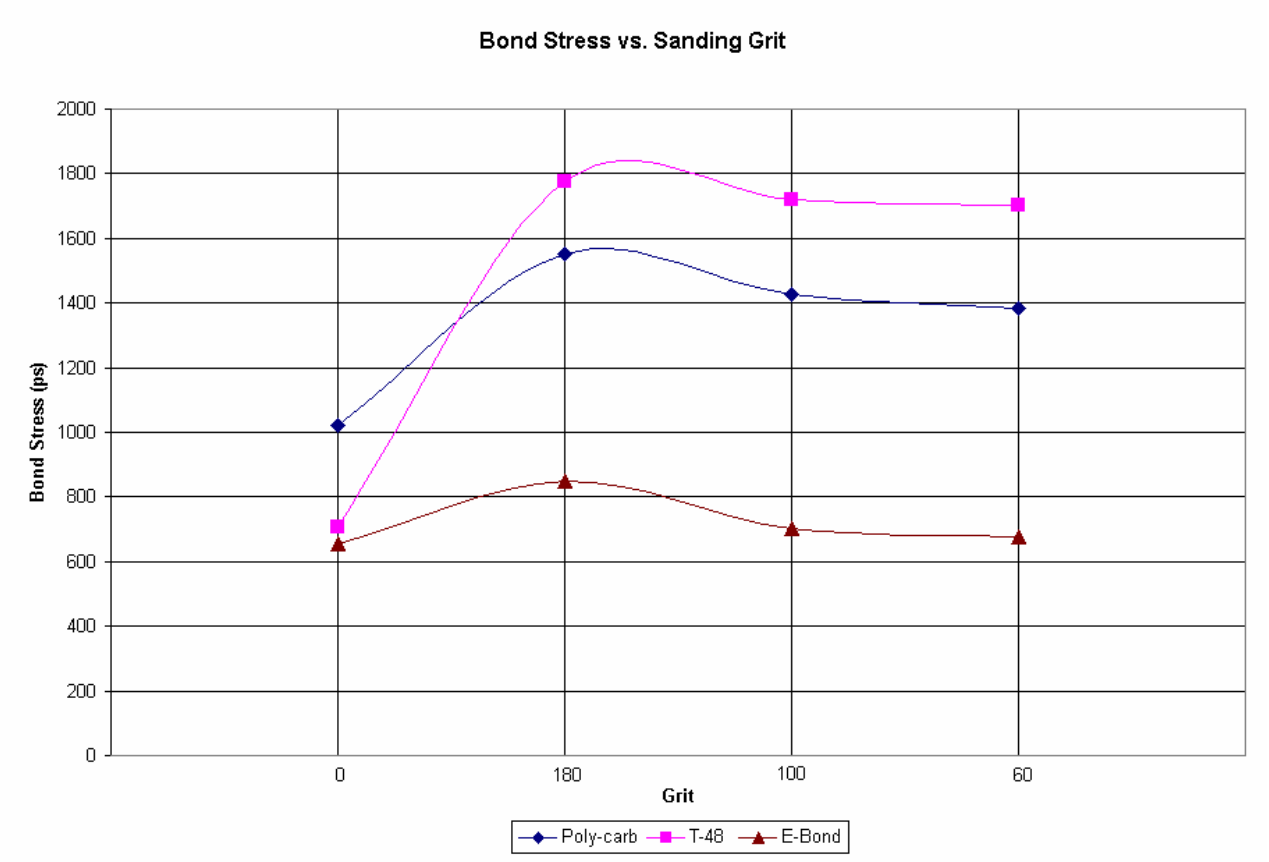

Figure 5.4.1: Bond stress vs. surface preparation level using various grit of sanding papers

Figure 5.4.2: Bond strength data for three resin binders with medium grade peel-ply surface.

5.5 Discussion & Conclusions

With no surface preparation, the failure occurred at the interface between the FRP and the polymer binder for all three resin binders. With surface preparation, the failure occurred in the vinyl ester resin used in the FRP for Polycarb Flexogrid Mark-163 and Transpo T-48. However, for E-Bond 526 the failure occurred in the interface for all samples. Therefore, in order to compare the three binders one must compare the failure stress with no surface preparation. This is because they fail in the same mode without surface preparation but in different modes with surface preparation. It is not appropriate to compare the bond stress with surface preparation for the Polycarb or T-48, which failed in the FRP, with that for E-Bond, which failed in the interface. The exact bond strength is not known for the Polycarb or T-48 sample with surface

preparation. The results obtained from samples without surface preparation showed that Polycarb has the highest bond strength (1010 psi) followed by T-48 (700 psi) and E-Bond (650 psi).

The curves for T-48 and Polycarb show a peak at the finest grit sand paper (i.e 180 grit) and then slightly go down with a rougher level of surface preparation. This observation may be ascribed to that using rougher grit sand paper removes more of the cover material from the FRP, resulting in the FRP having less strength and fails at a slightly lower load. Using rougher higher grit sandpaper also leaves the surface of the FRP with deeper groves, therefore creating stress concentrations at the high points in these groves. This also explains why the failure stress for the E-bond becomes slightly lower with rougher grit sandpapers. The results obtained from samples with surface preparation showed that T-48 has the highest failure strength (1800 psi) followed by Polycarb (1570 psi) and E-Bond (850 psi). The increase in failure strength is significant, as compared to no surface preparation, 150 % higher for T-48, 50% higher for Polycarb, and 30% higher for E-Bond. In this sense, T-48 and Polycarb overlay systems are much better than E-Bond 526 system. The result also suggests that a not-well prepared surface will result in weak bonds leading to premature failure.

For the FRP plates with medium grade peel-ply surfaces, all the polymer binders failed in the FRP. As shown in Figure 5.4.2, three replication tests for each resin binder yield consistent bond strength values, giving average bond strength of 880 psi for Poly-Carb, 840 psi for T-48 and 670 psi for E-Bond. These values agree rather well with the results for the FRP plates without surface preparation than those for the FRP panels with sanded surfaces. In particular, the bond strength values from the peel-ply method are about half of those from the sanding paper method for Polycarb or T-48. In addition, the peel-ply method appears to be not sensitive to chemical types of resin binders, all falling into a 30% window. Therefore, the comparison result between sanding method and peel-ply method supports the point that use of proper grit-blasting in preparing a surface for bonding is more reliable in field than creating a composite surface by removing a peel ply and the latter may lead to weak bonds possibly leading to premature failure.

On the other hand, as compared to those using different sand papers, the peel-ply does allow for quicker preparation because all you have to do is to peel the layer of fabric off the FRP surface and it is ready to apply the wearing surface. In contrast to the above, if using sanding method, you would have to first sand the surface taking special care to insure the entire surface

was sanded evenly, and then clean the surface to remove any dust particles from the sanding and any oils or other contaminants possibly from the sanders' skin, boots, etc. The latter process amounts to a longer period of time and greater cost but yield a significant increase in bond strength.

In conclusion, the relationship between the bond strength and surface preparation level established in this study suggests that a very fine grit sanding and proper cleaning is sufficient to yield good bond strength and a coarser grit sanding does not necessarily give better bond strength. At the same level of surface preparation, T-48 resin binder and Polycarb resin binder give much stronger bonds with FRP than E-Bond 526. As compared to the results from sanding method, the peel-ply method gives much lower bond strength but presents some field-operation advantages due to ease of use and the ability to get a good even preparation.

To enhance the bond strength with peel-ply FRP panels, we propose to apply a very thin layer of vinyl ester as primer after peeling off the cloth ply and before placing the resin binder. We also wish to evaluate other grades of peel-ply layers with different roughness so that we are able to examine the trend how the bond strength varies with the roughness of peel-ply. Evaluation of the proposed samples has already been carried out and some results are appended in Appendix A.

6. FIELD OBSERVATIONS OF POLYMER CONCRETE WEARING SURFACES ON FRP BRIDGE DECKS

6.1 Introduction

This chapter will present the field observations conducted and their relevance to the present study. The reader must keep in mind that the failures of PC discussed in this chapter are relative and when put into perspective with the success of PC these issues become a need for improving performance rather than a need for fixing performance problems. Even a few FRP bridges have experienced some minor cracking or small localized delaminations of their PC wearing surfaces, these bridges are still considered to be successes for PC in that the same minimal problems are being experienced with the use of other wearing surfaces such as 2" thick asphalt overlay, but the asphalt wearing surface contributes a significant extra amount of weight when compared to the PC overlay. More success stories of FRP bridges can be found in references (see for example, Justice, 2004; Reeve, 2001; Soneji, et al., 2001; Robert, 2001; FHWA, 2001; FHWA 2003; O'Connor, 2004; O'Connor, 2001; Whipp, 2001; Werts, 2001; Ray Publishing, 1997). For example, the polymer concrete overlays on Laurel Lick and Wickwire Run Bridges have been in use for seven years now and have only minimal surface cracking to speak of.

6.2 Problems In The Field

To date there have been numerous FRP bridge deck systems installed and in use in West Virginia. These deck systems have performed to expectations. However, several of these decks are experiencing cracking and delamination problems associated with their Polymer Concrete wearing surfaces. Three of theses bridges were visited during this project: Katy Truss Bridge, La Chein Bridge, and Market Street Bridge. The following is a summary of the background of the bridges and thoughts on what may be causing the problems. It is important that these failures do not constitute a failure in the bridge, a threat to motorist, nor a significant threat to the deck itself. The Katy Truss and Market Street Bridges utilize Creative Pultrusion's Superdeck^{TM} and the La Chein Bridge utilizes Bedford Reinforced Plastic's Decking system. The bridge specification provided below come form *Fiber Reinforced Polymer Composite Bridges of West*

Virginia a compilation by the Constructed Facilities Center of West Virginia University (FHWA, 2001).

6.2.1 Katy Truss Bridge

The Katy Truss Bridge, Fairmont, WV was finished in July of 2001. The bridge consists of a FRP deck on steel floor beam with steel truss/girders. It is a single span bridge with a 90 foot long by approximately 14 foot wide deck. The module to module connection was accomplished using pliogrip adhesive along with galvanized steel bind bolts. Polycarb was used as the resin binder for the 3/8" thick polymer concrete overlay.

Delamination of wearing surface was the biggest problem that occurred with the Katy Truss Bridge (Figure 6.2.1.1). Sections of the polymer concrete overlay could literally be lifted up and removed by hand. The Katy Truss Bridge also experienced some delamination of the fiber mats used to reinforce the field joints. The delamination is currently attributed to poor cleaning, preparation of the surface before placement of the PC overlay, and sloppy workmanship. This is the worst failure of PC encountered in West Virginia. Again it must be stressed, that this failure does not constitute a threat to motorist. The reader must also keep in mind is that the Average Daily Traffic on the Katy Truss Bridge is higher than was expected.

Figure 6.2.1.1: Delamination the wearing surface on the Katy Truss Bridge.

Figure 6.2.1.2: Delamination of FRP mat used to reinforce the field joint on Katy Truss Bridge.

6.2.2 La Chein Bridge

The La Chein Bridge, Monroe County, WV was constructed in August 2002. It consists of a FRP deck on steel stringers with a 25˚ skew. The bridge is a single span bridge with an approximately 41 foot long by 24 foot wide deck. Pliogrip adhesive was used for the module to module connections. Transpo T-48 was used as the resin binder for the overlay.

Cracking of the polymer concrete overlay followed by visible delamination has occurred on the La Chein Bridge. This cracking occurs over the module joints (Figure 6.2.2.1 thru Figure 6.2.2.5). The cause of this cracking is not yet known. It is suspected that the cracking occurred due to poor bond between the FRP deck and the PC overlay and/or reflective cracking due to the thermal gradient experienced by the deck, which would result in the PC overlay cracking. These failures do not present a threat to motorist or the deck. The following figures are courtesy of WVDOT Engineers.

Figure 6.2.2.1: A crack located on La Chein Bridge.

Figure 6.2.2.2: Close up of a crack on La Chein Bridge.

Figure 6.2.2.3: Cracking and delamination on La Chein Bridge.

Figure 6.2.2.4: Cracking and delamination on La Chein Bridge.

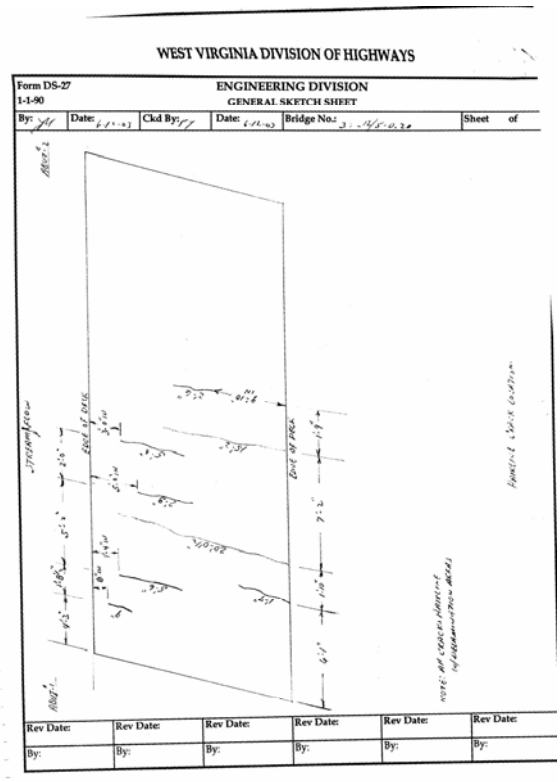

Figure 6.2.2.5: Location of cracks on La Chein Bridge.

6.2.3 Market Street Bridge

The Market Street Bridge, Wheeling, WV was finished in July of 2001. It consists of a FRP deck on steel plate girders. The bridge is a single span jointless bridge with an approximately 180 foot long by 56 foot wide deck. Pliogrip adhesive was used for the module to module connections. Polycarb was used as the resin binder for the polymer concrete wearing surface.

Minor cracking of the polymer concrete overlay has occurred on this bridge, mainly over the field joint but also over the manufacturer module joints (Figure 6.2.3.1 thru Figure 6.2.3.4). The cause of this cracking is not yet known. It is suspected that the cracking occurred due to the braking forces of large trucks and vehicles, since the frequency and size of the cracks increase toward the northeast side of the bridge where a stoplight is located. It is also suspected that the crack concentration in the center is due to the additional forces imposed by heavy trucks breaking and changing lanes at the same time. Again it can not be stressed enough that these

failures do not present a threat to motorist or the deck.. As a matter of fact, this FRP composite bridge has been performing extremely well.

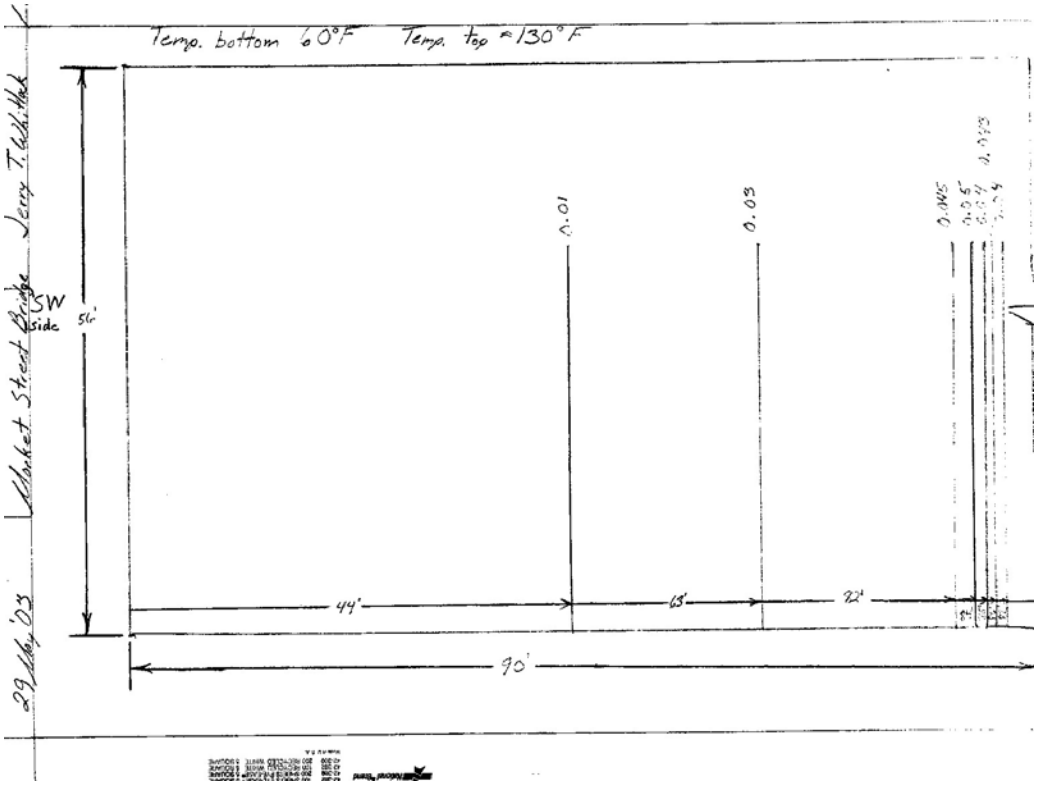

Figure 6.2.3.1: Crack locations and sizes on Market Street Bridge section 1.

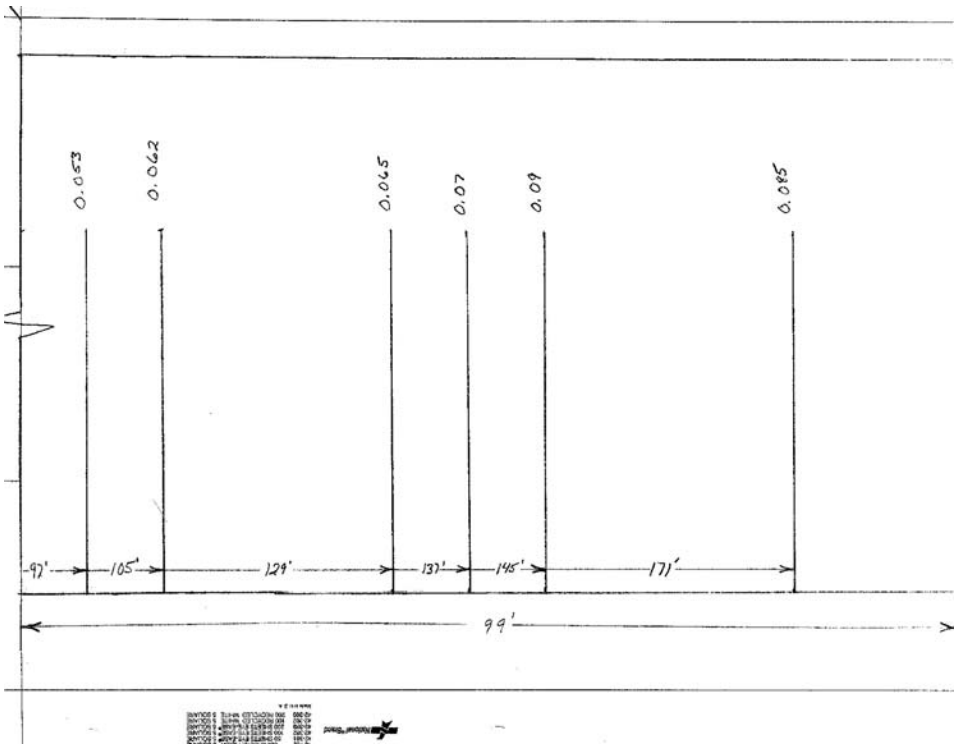

Figure 6.2.3.2: Crack locations and sizes on Market Street Bridge section 2.

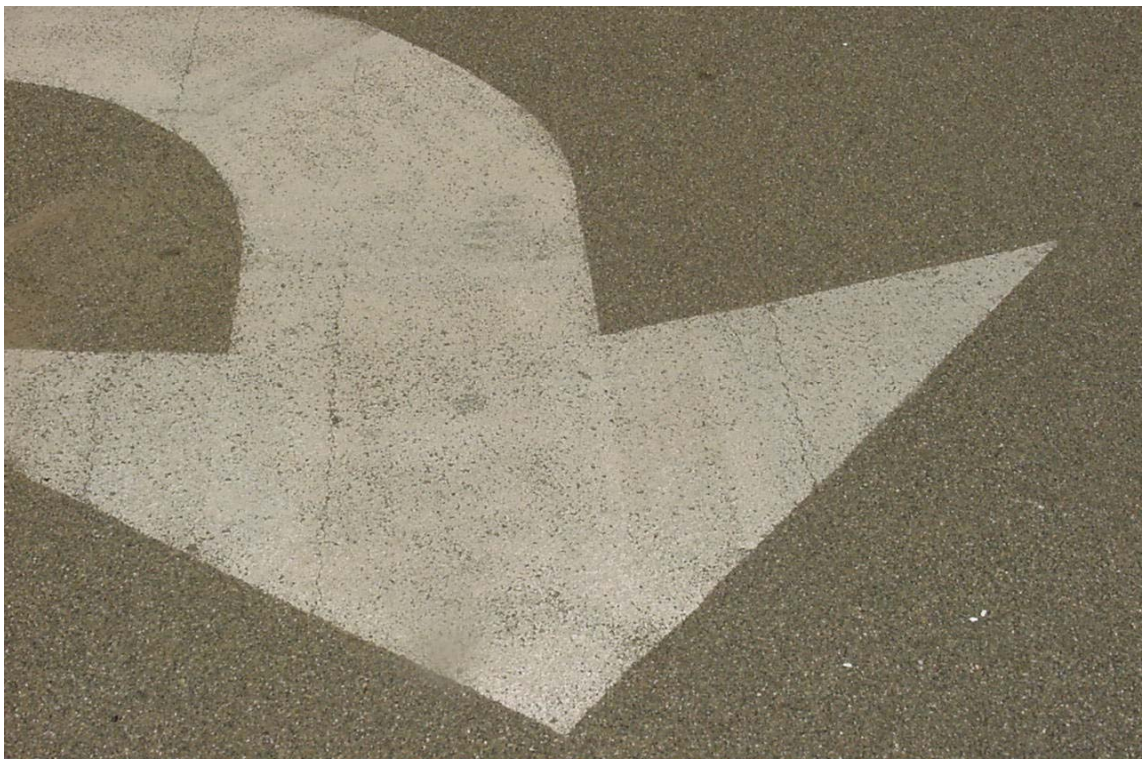

Figure 6.2.3.3: Surface Cracks in PC overlay, Market Street Bridge.

Figure 6.2.3.4: Surface Cracks in PC overlay, Market Street Bridge.

6.3 Discussion and Conclusions

It is intended to correlate the findings of this study with field observation of existing wearing surfaces on FRP bridge decks. Thermal compatibility, strain compatibility, and interfacial bond strength are believed to be the primary reasons that polymer concrete wearing surfaces fail. However, the knowledge and findings accomplished through the present investigation do not provide a direct solution to any of the above field problems.

Poly-Carb was used as a resin binder of 3/8" thin wearing surface for both Market Street Bridge and Katy Truss Bridge at the same time –July 2001. Katy Truss bridge decks developed waering surface problems with large area of the polymer concrete delaminating from the FRP deck, whereas Market Street bridge decks had no problems except some minor cracking mostly along the joints of FRP deck modules. La Chein Bridge with Transpo T-48 overlays was constructed in August 2002, but its FRP decks had delamination problems with the original wearing surface in June 2003 (Lusk, 2003). Those delamination problems developed most possibly during the first winter season.

Property measurement of a given polymer concrete in the laboratory is conducted under a well- controlled environment as compared to complicated field conditions. For example, the field trip to Market Street Bridge took place on May 29, 2003. The weather on that day was sunny with some clouds. A surface temperature of 130F was detected for FRP decks while the temperature under the bridge was only 60F, giving a temperature difference of 70F. Therefore, the material sections at different depths were subjected to non-uniform thermal field, leading to different thermal expansion and stress level. Similar thermal process is occurring every day. Day after day's accumulation from these thermal expansion and contract could result in permanent deformation or distortion, leading to cracking. Therefore, field evaluation of existing FRP bridges are very important in order to understand problems and should be continued. It is noted that New York State DOT is teaming up with researchers at Syracuse University and Cornell University to determine acceptable wearing surface product for FRP decks in NYS (Yannotti, et al., 2004).

The success of PC overlays in West Virginia far outs way the failures. For example, on the bridges presented above the PC was still an overall success because the primary reason for using PC as an overlay on FRP bridge decks was to provide a light weight wearing surface with adequate skid resistance. The secondary requirement for the PC Overlay was to protect the FRP Deck. The Katy Truss Bridge is the only one that is a borderline failure of this secondary requirement. However, due to approximately 80% of the deck still being covered with the PC overlay and the exposed area of the bridge showing no signs of damage the overlay, although in need of replacement, is not an overall failure.

7. CONCLUSIONS & RECOMMENDATIONS

7.1 Introduction

This chapter will present the conclusions drawn form the present experimental work as well as the recommendations for further testing and evaluation.

7.2 Conclusions

The present experimental study demonstrates that all three polymer concrete wearing surface systems tested performed satisfactorily with FRP. As seen in Table 7.2.1, Transpo T-48 PC overlay system has the lowest CTE and thus is the most compatible with FRP, followed by E-Bond 526 and Polycarb Mark 23. However, E-Bond 526 showed a smaller difference in interface strain between FRP and the PC overlay and therefore has a better stain compatibility with FRP, followed by Transpo T-48 and Polycarb Mark 23. Considering energy absorption/strain slippage, Transpo T-48 has the highest energy absorption, followed by Polycarb Mark 23 and E-Bond 526. Transpo T-48 has the highest bond strength, followed by Polycarb Mark 23 and E-Bond 526.

As a result of this study, Transpo T-48 is identified to be the most compatible overlay system for glass FRP deck applications. Poly-Carb Mark 163 has significant advantages over E-Bond 526 in the sense of bond strength and energy absorption capacity, whereas E-Bond 526 has exhibited better thermal and strain compatibility at the interface of PC and FRP deck than Poly-Carb Mark 163.

The investigation indicates that a very fine surface preparation (enough to remove the shine from the surface of FRP) in conjunction with good cleaning is all that is needed to yield sufficient bond strength development. With a fine grit sanding, the bond strengths for three resin binders are: 1800 psi with T-48, 1570 psi with Polycarb, and 850 psi with E-Bond. As compared to the results from grit paper sanding method, the peel-ply method gives much lower bond strength but presents some field-operation advantages due to ease of use and the ability to get a good even preparation. With a medium peel-ply, the bond strengths are 880 psi for Poly-Carb, 840 psi for T-48, and 670 psi for E-Bond. Whether these bond strengths are sufficient enough to avoid premature failure has to be addressed.

Table 7.2.1: Summary of Results.

	CTE		Strain Compatibility		Bond Strength	
	Neat Resin	PC	Compatibility	Energy Absorption	Sanding	Peel-Ply
	10E^-6 in/in/F				psi	
Poly Carb	12.67 ± 2.14	10.38 ± 0.7	Good	High	1570	930
T-48	10.07 ± 0.49	8.09 ± 0.24	Good	High	1800	990
E-Bond	8.87 ± 1.03	8.40 ± 0.38	Best	Low	850	700

7.3 Recommendations

The following recommendations are made from this study: 1) evaluation of the use of vinyl ester resin as the binder in order to achieve a better property matching between the FRP and PC overlay; 2) evaluation of the use of a primer coat of vinyl ester when the peel-ply method is used; 3) evaluation of different peel-ply grades for the peel-ply method; 4) evaluation of different materials for use over the field joints; and 5) use of the peel-ply method of surface preparation in conjunction with proper cleaning for field applications, ensuring that the PC overlay is applied as soon as possible after the removal of the peel-ply and cleaning of the surface.

BIBLIOGRAPHY

AASHTO (1995) "Guide Specifications for Polymer Concrete Bridge Deck Overlays," American Association of State Highway and Transportation Officials, AASHTO-AGC-ARTBA Task Force 34 Report, Washington, DC

AASHTO SHRP Product 2035B (1999) "Guide Specifications for Polymer Concrete Bridge Deck Overlays," AASHTO, Washington, DC
http://leadstates.tamu.edu/car/SHRP_products/2035b.stm

ACI 548.5R-94 (1994) "Guide for Polymer Concrete Overlays," American Concrete Institute ACI Committee 548 Report, Detroit, MI

Black, Sara. (2003) "How Are Composite Bridges Performing?" Composite Technology, December 2003, pp.16-22

Cassity, Patrick A. (2000) "Fiber-Reinforced Polymer Bridge Decks," August 5, 2000, J. Muller International, Chicago, IL
http://www.nabro.unl.edu/articles/20000805/index.asp

Deitz, David Holman. (2002), "FRP Improves Bridge Deck Life," Better Roads Magazine, November 2002 http://www.betterroads.com/articles/nov02d.htm

Deshpande, Rahul. (1992) "Wearing Surface Testing of Modular Fiberglass Deck System," Graduate Research Study Report (Cal State U Long Beach), FHWA Turner Fairbank Highway Research Center, Mc Lean, VA

E-Bond 526 Users' Guide (2000) "Proposed Special Provision Epoxy Polymer Multiple Layer Waterproofing Overlays for Bridge Decks," E-Bond Epoxies, Inc. Fort Lauderdale, FL

FHWA. (2001) "Fiber Reinforced Polymer Composite Bridges of West Virginia," U.S. DOT/FHWA, Publication No: FHWA-ERC-2-002

FHWA. (2003) "Fiber Reinforced Polymer Bridge Decks of New York," New York State's FRP Bridge Applications, Spring 2003

Justice, Jack (2004) "West Virginia Fiber Reinforced Polymer Case Studies", Pre-Conference Short Course: Case Studies in Uses of Composites in Infrastructure Applications, March 30 04, Morgantown, WV

Liang, Ruifeng, Abhishek Anjanappa, Hota GangaRao, and Rakesh Gupta. (2001) "Mechanical and Thermal Properties of Alloys at Elevated Temperatures," Technical Report to USDOE-NETL, Constructed Facilities Center, West Virginia University, Morgantown, WV

Lopez-Anido, Roberto, Dustin Troutman, and John P. Busel. (1998) "Fabrication and Installation of Modular FRP Composite Bridge Deck," Proceedings of International Composites Expo (ICE-98, Nashville, TN, Jan 19-21), Session 4-A, pp.1-6

Lopez-Anido, Roberto, Hota V.S. GangsRao, Richard J. Pauer, and Venkata R. Vendam. (1998) "Evaluation of Polymer Concrete Overlay for FRP Composite Bridge Deck," Proceedings of International Composites Expo (ICE-98, Nashville, TN, Jan 19-21), Session 13-F, pp.1-6

Lusk, Adrian. (2003) Discussions on La Chein Bridge Wearing Surface, Private Communications, District Nine, Bridge Department, WVDOT, Charleston, WV

MDA. (2003a) "FRP Bridge Product Gateway: Vehicle Bridge Decks," Market Development Alliance of the FRP Composites Industry http://www.mdacomposites.org/PSGbridge_Vehicular_intro.html

MDA. (2003b) "Global FRP Use for Bridge Applications," Market Development Alliance of the FRP Composites Industry, April 1 2003 http://www.mdacomposites.org/bridge_statistics.htm

Moretti, Frank and Paul Haaland. (2002) "One in Four Bridges in U.S. is Deficient; Average Age of Bridges in U.S. is Forty," TRIP- The Road Information Program, May 7 2002 http://www.tripnet.org/national.htm

O'Connor, Jerome S. (2001), "New York's Experience with FRP Bridge Decks," Polymer Composites II: Applications of Composites in Infrastructure Renewal and Economic Development, ed. by R. Creese & H. GangaRao, pp.21-32, CRC press: Washington, DC

O'Connor, Jerry. (2003) "FRP Decks and Superstructures: Current Practice," U.S. DOT/FHWA – Bridge Technology, October 27, 2003, http://www.fhwa.dot.gov/BRIDGE/frp/deckprac.htm

Ray Publishing. (1997) "FRP Decks Complete Two West Virginia Bridges," Composites Technology: Engineering and Manufacturing Solutions for Industry, July/August 1997 Issue, pp.5-7

Reeve, Scott R. (2001) "FRP Composite Bridge Decks: Barriers to Market Development," Polymer Composites II: Applications of Composites in Infrastructure Renewal and Economic Development, ed. by R. Creese & H. GangaRao, pp.180-186, CRC press: Washington, DC

Reeve, Scott R. (2003) "FRP Bridge Decks: Inspecting for the Future," Composite Fabrication, April 2003 Issue, p.40

Reeve, Scott and Ela Kos (2004) "FRP Composite Bridge Decks: National Composite Center Experiences", Polymer Composites III 2004: Transportation Infrastructure, Defense and Novel

Applications of Composites, ed. by R. Creese & H. GangaRao, pp.99-108, DES Tech Publications: Lancaster, PA

Robert, Jeffrey L. (2001) "Replacement of the Bridge on MD24 over Deer Creek in Hartford County, Maryland, Utilizing a Fiber-Reinforced Polymer (FRP) Deck", Polymer Composites II: Applications of Composites in Infrastructure Renewal and Economic Development, ed. by R. Creese & H. GangaRao, pp.43-57, CRC press: Washington, DC

Scott, Irene and Ken Wheeler. (2001) "Application of Fibre Reinforced Polymer Composites in Bridge Construction," NSW IPWEA State Conference 2001 - 17 October, Port Macquarie, Australia
http://www.ipwea.org.au/papers/download/Irene%20Scott.doc

Solomon, Greg. (2002) "DuraSpan Fiber-Reinforced Polymer Bridge Deck Systems," Martin Marietta Composites Brochure, Raleigh, NC.
http://www.martinmarietta.com/Products/Duraspan.pdf

Soneji, J, C. Hu, M. Chaudhri, A. Faqiri, J. W. Gillespie Jr., D. A. Eckel II, D. R. Mertz, M. J. Chajes. (2001) "Use of Glass-Fiber-Reinforced Composite Panels to Replace the Superstructure for Bridge 351 on N387A Over Muddy Run," Polymer Composites II: Applications of Composites in Infrastructure Renewal and Economic Development, ed. by R. Creese & H. GangaRao, pp.3-20, CRC press: Washington, DC

Sprinkel, Michael. (2001) "Twenty-Five-Year Experience with Polymer Concrete Overlays on Bridge Decks," Polymer Composites II: Applications of Composites in Infrastructure Renewal and Economic Development, ed. by R. Creese & H. GangaRao, pp.58-69, CRC press: Washington, DC

Stewart, Richard. (2002) "U.S. Composites Industry Expands Despite Economy," Reinforced Plastics, Nov. 2002 Issue, p.20-26

Vendam, Venkata R. (1997) "Characterization of Composite Material Bridge," M.S Thesis, Constructed Facilities Center, West Virginia University, Morgantown, WV

VDOT Guidelines (1993) "Special Provision for Epoxy Concrete Overlay," February 3, 1993, Virginia Department of Transportation, Richmond, VA

VTM-92. (1993) "Virginia Test Method for Testing Epoxy Concrete Overlays for Surface Preparation and Adhesion," Virginia Department of Transportation, Richmond, VA

Werts, William M. (2001) "PennDOT's First FRP Deck," Polymer Composites II: Applications of Composites in Infrastructure Renewal and Economic Development, ed. by R. Creese & H. GangaRao, pp.33-42, CRC press: Washington, DC

Whipp, Robert W. (2001) “Constructing the Market Street Bridge,” Polymer Composites II: Applications of Composites in Infrastructure Renewal and Economic Development, ed. by R. Creese & H. GangaRao, pp.117-69, CRC press: Washington, DC

Yannotti, Arthur P. and Alampalli Sreenivas (2004) “New York’s Experience with FRP Materials for Bridge Applications”, Polymer Composites III 2004: Transportation Infrastructure, Defense and Novel Applications of Composites, ed. by R. Creese & H. GangaRao, pp.17-26, DES Tech Publications: Lancaster, PA

APPENDIX A
BENDING TEST OF FRP PANELS WITH PLANT CAST WEARING SURFACES

A.1 Introduction

In light of those findings from this study, further investigation of wearing surfaces prepared with variable peel-ply grades and the use of vinyl ester resin as a binder has been recommended in Chapter 7 of this report. In collaboration with Bedford Reinforced Plastics (BRP) Inc, Bedford, PA, FRP deck panels coated with wearing surfaces of the above variations have been manufactured and are being evaluated through bending tests. Since these new samples were produced by the manufacturer, the testing methods used previously are not applicable to these samples, therefore, resulting in the inability to directly compare any new result with previous results. Instead, these new samples will be subjected to thermal gradient testing and accelerated aging test. The samples are being placed inside an environmental chamber and subjected to various thermal aging cycles before testing. Then the results will be discussed with reference to previous findings. This appendix will summarize the results from bending tests of these as-received samples.

A.2 Specimen Preparation and Test Method

Two types of wearing surfaces were plant-cast on FRP deck panels at BRP Inc and delivered to CFC-WVU for evaluation. One type of wearing surfaces was constructed with Transpo T-48 epoxy resin using three peel-ply grades (Test 1 representing a fine peel ply, Test 2 – a medium peel ply, and Test 3 – a coarse peel ply). Basalt aggregate was used in conformation with T-48 application guidelines. The other type of wearing surfaces was constructed with vinyl ester as the binder and two kinds of aggregates, i.e. basalt aggregate and quartz aggregate using a medium grade of peel ply.

The as-received samples of varying peel ply grades have dimensions of 2 inch wide by approximately 1 inch thick by 24 inch long and are made of ½” thick FRP panel and 5/16” to 3/8” thick overlay. The as-received samples of varying aggregates have dimensions of 1 inch wide by approximately 1 inch thick by 24 inch long and are made of ½” thick FRP panel and

3/16” to 1/4” thick overlay. But all the testing specimens were cut into dimensions of 1 inch wide and 14 inch long. Strain gauges were placed and centered on the top and bottom of the specimens. The specimens were then tested under a three point bending setup with a span length of 9 inches.

A.3 Results

A.3.1 Variable Peel-Ply Roughness

The strain variation diagrams presented in this section were obtained by assuming that the strain at the interface between FRP and PC is approximately equal to the negative of the strain at the bottom of the FRP. This assumption is valid because the FRP resists almost all applied moment with the moment resisted by the PC being negligible.

A.3.1.1 Fine Grade Peel-Ply

Table A.3.1.1.1 Strain data for fine grade peel-ply sample bending test.

	Load (lbs)	Strain Top * 10^-6	Strain Bottom * 10^-6
Sample 1			
	0	0	0
	100	-3056	2365
	200	-6421	4945
	300	-8505	7593
	400	-10267	10116
	500	-11744	12113
	600	-11794	gauge failure
Sample 2			
	0	0	0
	100	-3042	2526
	200	-6550	5234
	300	-9452	8060
	400	-12958	10893
	500	-13863	14084
	600	-12788	16833
	700	-13991	gauge failure

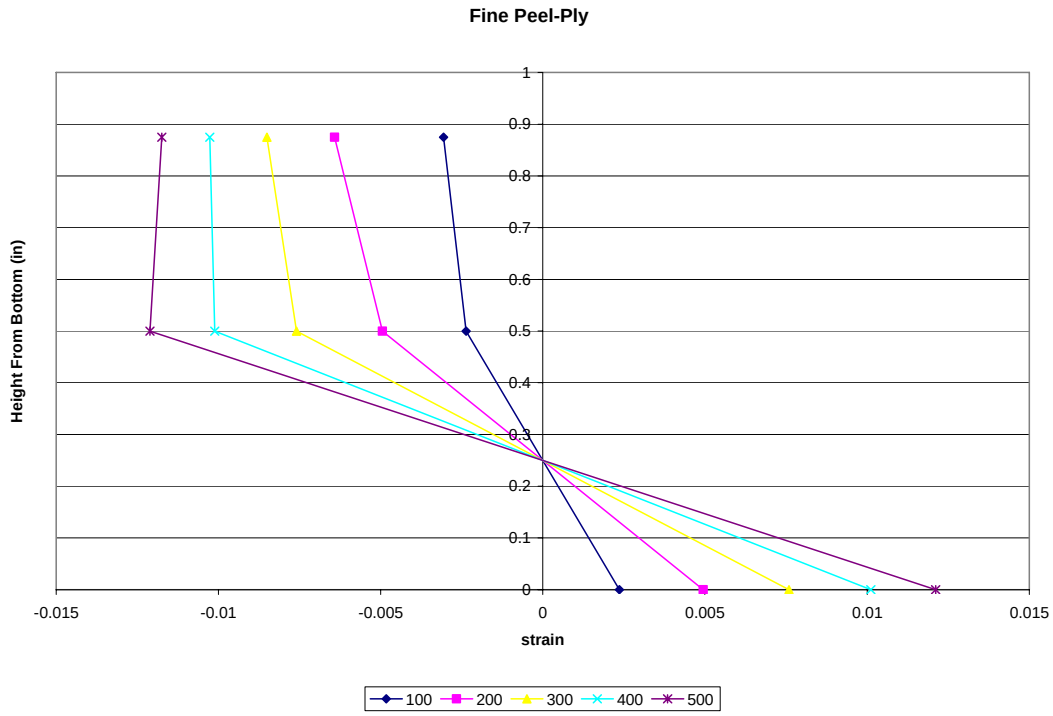

Figure A.3.1.1.1: Strain variation diagram for fine peel-ply sample.

A.3.1.2 Medium Grade Peel-Ply

Table A3.1.2.1: Strain data for medium grade peel-ply sample bending test.

	Load (lbs)	Strain Top * 10^-6	Strain Bottom * 10^-6
Sample 1			
	0	0	0
	100	-4946	2916
	200	-8503	5690
	300	-11315	7217
	400	-14010	8856
	500	-16320	9833
Sample 2			
	Pretest Gauge Failure		

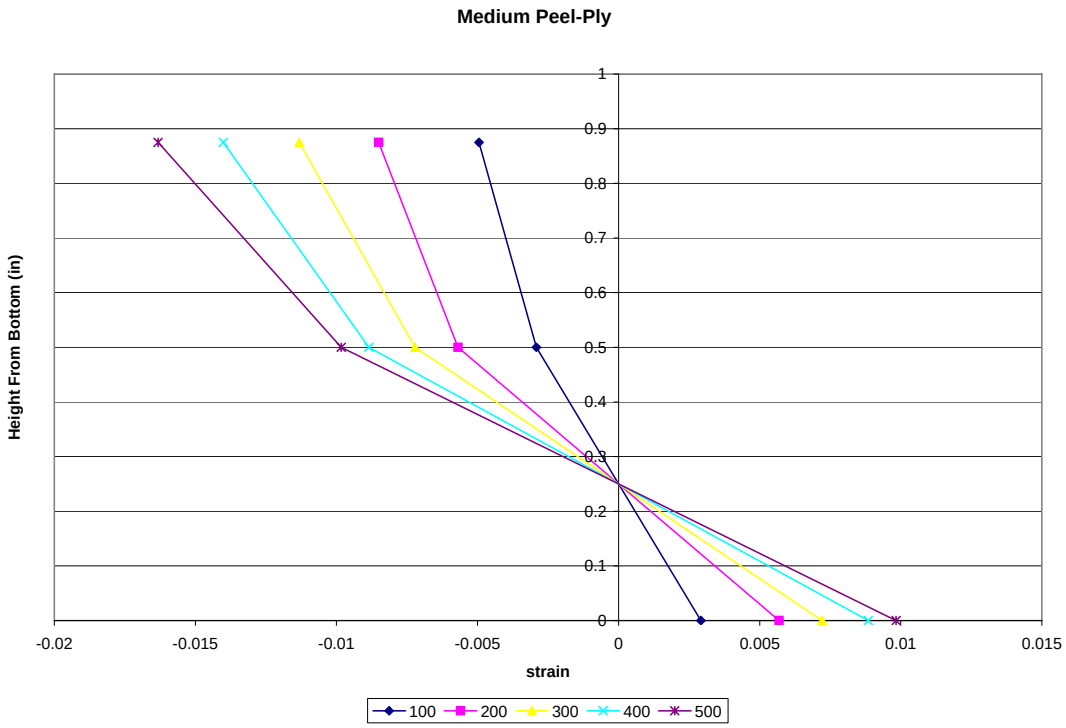

Figure A.3.1.2.1: Strain variation diagram for medium peel-ply sample.

A.3.1.3 Rough Grade Peel-Ply

Table A3.1.3.1: Strain data for rough grade peel-ply sample bending test.

	Load (lbs)	Strain Top * 10^-6	Strain Bottom * 10^-6
Sample 1			
	0	0	0
	100	-4204	2568
	200	-8146	5079
	300	-11706	7746
	400	-15656	10434
	500	-19019	11852
	600	-19978	gauge failure
Sample 2			
	0	0	0
	100	-3752	2249
	200	-7752	4642
	300	-10638	6745
	400	-13770	9131
	500	-16491	gauge failure

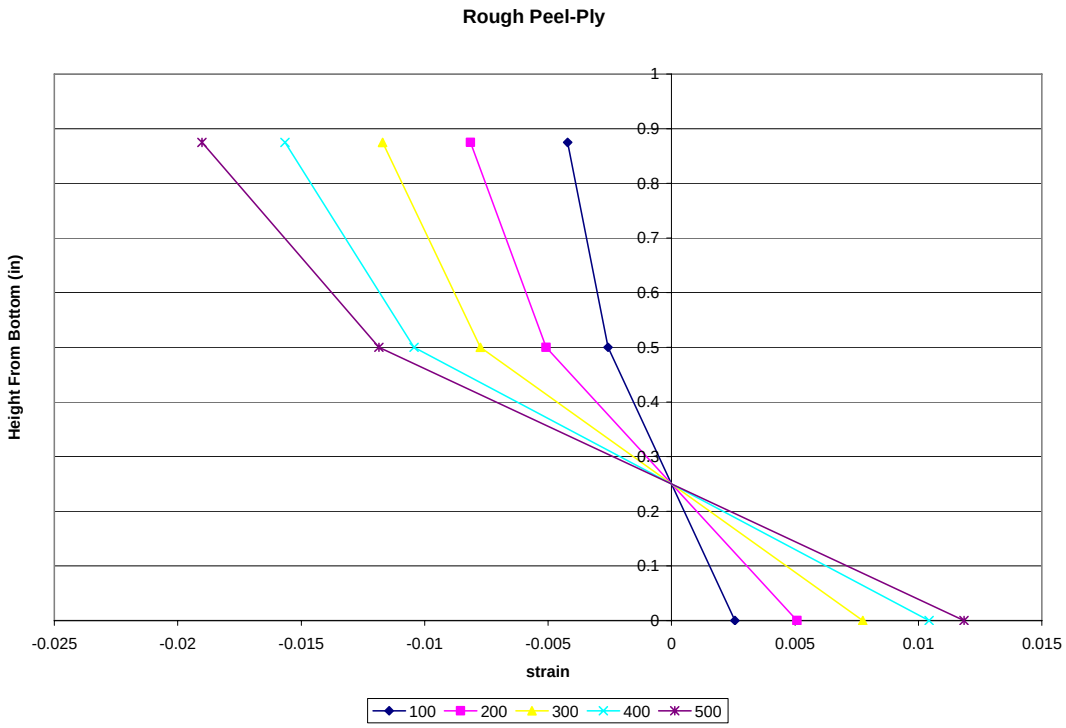

Figure A.3.1.3.1: Strain variation diagram for rough peel-ply sample.

A.3.2 Vinyl Ester Binder

A.3.2.1 Basaltic Aggregate

Table A3.2.1.1: Strain data from bending test for vinyl ester binder with basalt aggregate.

	Load (lbs)	Strain Top * 10^-6	Strain Bottom * 10^-6
Sample 1			
	0	0	0
	100	-1768	2984
	200	-3835	4550
	300	-5954	6285
	400	-8375	8045
	500	-10756	10108
	600	-14143	12285
	700	-17135	13534
	800	-19696	15009
Sample 2			
	0	0	0
	100	-1860	1506
	200	-3415	2848
	300	-5067	gauge failure
	400	-7000	

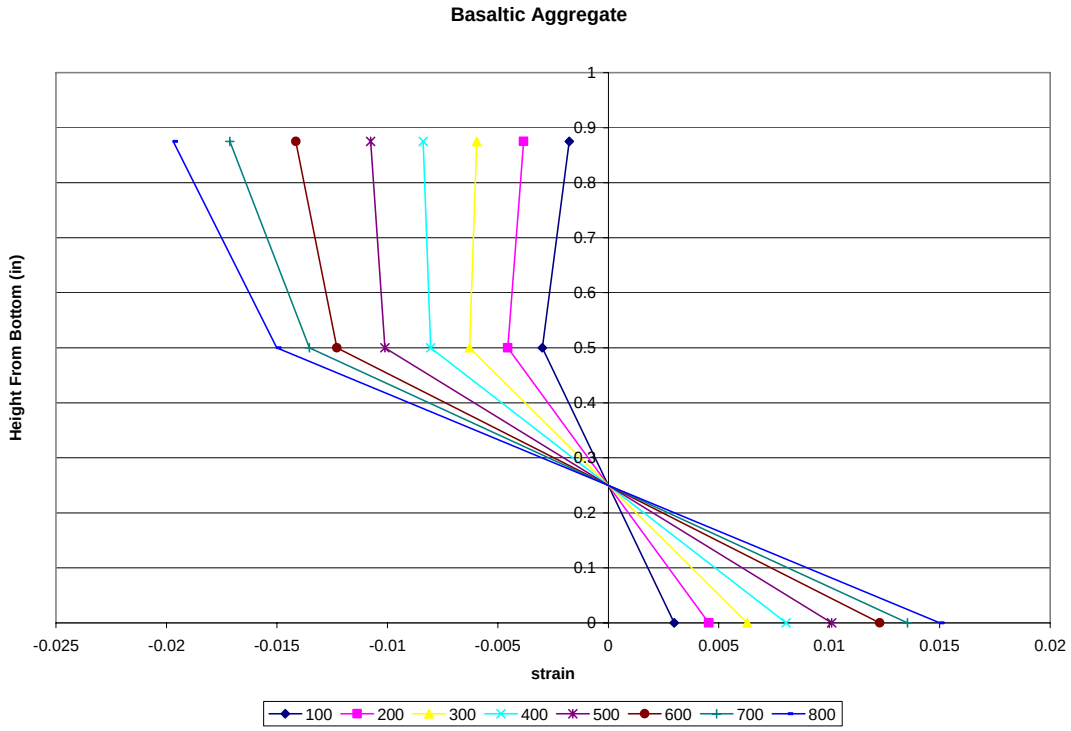

Figure A.3.2.1.1: Strain variation diagram for vinyl ester binder with basalt aggregate.

A.3.2.2Quartz Aggregate

Table A3.2.2.1: Strain data from bending test for vinyl ester binder with quartz aggregate.

	Load (lbs)	Strain Top * 10^-6	Strain Bottom * 10^-6
Sample 1			
	0	0	0
	100	-2751	1557
	200	-5105	3068
	300	-7050	4539
	400	-9866	6415
	500	-11715	7486
	600	-13430	9804
	700	-15160	11795
	800	-16774	13666
	900	-18506	15885
Sample 2			
	0	0	0
	100	-1385	1772
	200	-3273	1984
	300	-4659	3236
	400	-6334	5601
	500	-8235	6033
	600	-9961	gauge failure

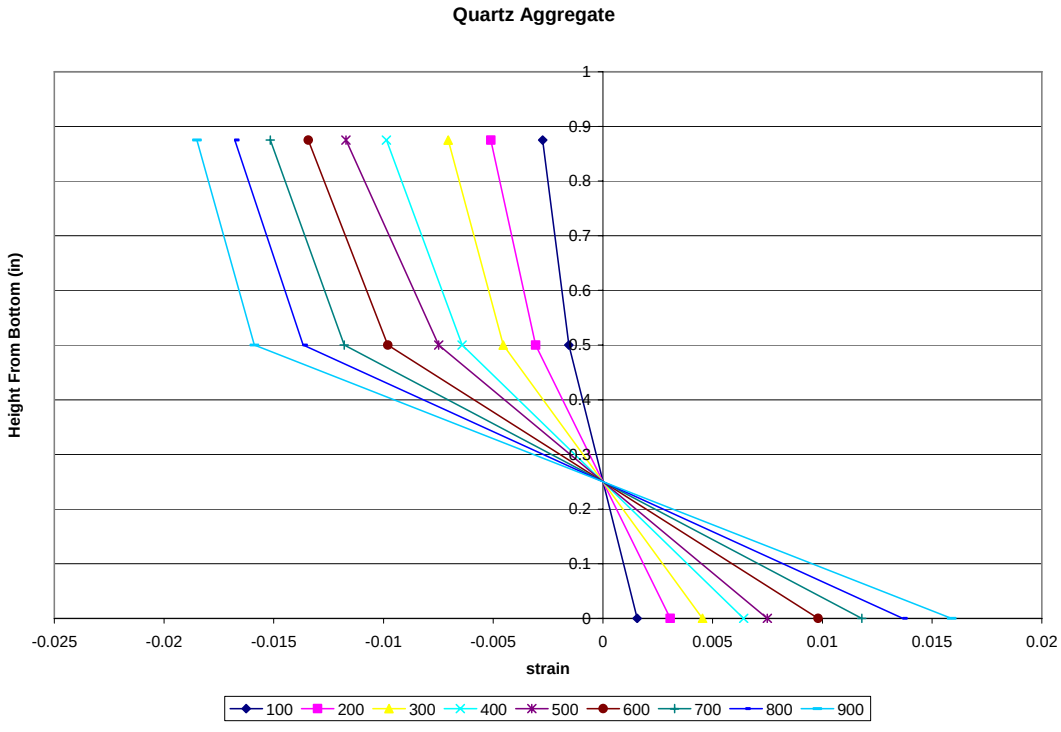

Figure A.3.2.2.1: Strain variation diagram for vinyl ester binder with quartz aggregate.

A.4 Conclusions

It can be concluded from the above diagrams that the rougher the peel-ply the smaller the amount of strain slippage and the better the strain compatibility with FRP, but the medium grade peel-ply shows almost the same result as the coarse grade peel-ply. With the same medium grade peel-ply, T-48 epoxy shows better the strain compatibility with FRP than vinyl ester as a binder. It appears that the quartz aggregate gives a slightly better strain compatibility with FRP than basalt aggregate, but two types of aggregates are essentially behaving the same. This is because aggregates are broadcast only on the top of resin mixture with fine sand.

APPENDIX B
RAW TEST DATA

B.1 Coefficient of Thermal Expansion Data

Table B.1.1: Raw CTE data for Poly-Carb Mark 163 neat resin.

	Temperature (˚F)	Strain *10^-6
Sample 1		
	75	4
	80	60
	90	240
	100	369
	110	552
	120	724
	130	764
	140	838
	150	963
	160	1056
Sample 2		
	120	165
	130	260
	140	350
	150	396
	160	487
	170	715
	180	806
Sample 3		
	85	260
	100	460
	120	813
	130	903

Table B.1.2: Raw CTE data for Poly-Carb Mark 163 polymer concrete.

	Temperature (˚F)	Strain *10^-6
Sample 1		
	93	40
	113	225
	129	441
	152	700
	166	815
	170	866
Sample 2		
	76	10
	93	196
	113	386
	132	592
	150	728
	163	846
Sample 3		
	90	3
	113	213
	128	406
	152	685
	163	769
	172	856

Table B.1.3: Raw CTE data for Transpo T-48 neat resin.

	Temperature (˚F)	Strain *10^-6
Sample 1		
	77	1
	96	168
	115	355
	133	520
	152	700
	162	825
Sample 2		
	104	30
	123	210
	140	435
	160	596
	167	703
Sample 3		
	75	10
	93	206
	113	445
	132	679
	152	762
	162	896

Table B.1.4: Raw CTE data for Transpo T-48 polymer concrete.

	Temperature (˚F)	Strain *10^-6
Sample 1		
	76	0
	93	100
	113	255
	132	440
	150	591
	163	642
Sample 2		
	75	30
	93	133
	113	286
	128	489
	132	507
	152	631
	162	709
Sample 3		
	105	12
	123	168
	142	297
	153	401
	162	498

Table B.1.5: Raw CTE data for E-Bond 526 neat resin.

	Temperature (˚F)	Strain *10^-6
Sample 1		
	115	177
	132	390
	140	488
	153	560
	167	654
Sample 2		
	95	10
	115	165
	123	295
	132	406
	142	495
	153	549
	162	661
Sample 3		
	105	54
	112	136
	132	257
	146	392
	162	506

Table B.1.6: Raw CTE data for E-Bond 526 polymer concrete.

	Temperature (°F)	Strain *10^-6
Sample 1		
	110	470
	135	700
	138	770
	165	910
Sample 2		
	95	30
	112	198
	133	316
	142	489
	160	597
Sample 3		
	115	60
	132	216
	142	299
	156	385
	163	482

B.2 Strain Variation Diagram Data

Table B.2.1: Strain data for Poly-Carb Mark 163 sample.

	Load (lbs)	Strain Top *10^-6	Strain Middle *10^-6	Strain Bottom *10^-6
Sample 1				
	50 lbs	-0.00043	-0.00041	0.000472
	100 lbs	-0.0008	-0.00075	0.000846
	200 lbs	-0.00157	-0.00141	0.001613
	250 lbs	-0.00201	-0.00178	0.00208
	300 lbs	-0.00234	-0.00221	0.002593
	350 lbs	-0.00273	-0.00268	0.003149
	400 lbs	-0.00311	-0.00301	0.003565
Sample 2	Gauge failure			

Table B.2.2: Strain data for Transpo T-48 sample.

	Load (lbs)	Strain Top *10^-6	Strain Middle *10^-6	Strain Bottom *10^-6
Sample 1				
	50 lbs	-0.00014	-0.00057	0.000637
	100 lbs	-0.00025	-0.00104	0.001133
	200 lbs	-0.00041	-0.00201	0.002187
	250 lbs	-0.00049	-0.00281	0.0029
	300 lbs	-0.00056	-0.00336	0.003583
	350 lbs	-0.00068	-0.00436	0.004823
	400 lbs	-0.00076	-0.0052	0.005784
Sample 2	Gauge failure			

Table B.2.3: Strain data for E-Bond 526.

	Load (lbs)	Strain Top *10^-6	Strain Middle *10^-6	Strain Bottom *10^-6
Sample 1				
	50 lbs	-0.00051	-0.00048	0.00049
	100 lbs	-0.00074	-0.00103	0.00107
	200 lbs	-0.00107	-0.00205	0.002164
	250 lbs	-0.00124	-0.0028	0.002932
	300 lbs	-0.00135	-0.00329	0.00348
	350 lbs	-0.00148	-0.00428	0.00463
	400 lbs	-0.00155	-0.00483	0.005449
Sample 2				
	50 lbs	-0.00025	-0.00043	0.000523
	100 lbs	-0.00047	-0.0009	0.001064
	200 lbs	-0.00092	-0.0016	0.001883
	250 lbs	-0.00113	-0.00219	0.002563
	300 lbs	-0.00132	-0.00276	0.00323
	350 lbs	-0.00147	-0.00315	0.003678
	400 lbs	-0.00166	-0.00366	0.004339

B.3 Bond Strength Data

Table B.3.1: Bond strength data for Poly-Carb Mark 163 sample.

Sample	Max Load (lbs)
0-1	1252
0-2	1269
180-1	1891
180-2	1902
100-1	1706
100-2	1750
60-1	1685
60-2	1698

Table B.3.2: Bond strength data for Poly-Carb Mark 163 with peel ply surface preparation.

Sample	Max Load (lbs)
1	940
2	1135
3	1131

Table B.3.3: Bond strength data for Transpo T-48 sample.

Sample	Max Load (lbs)
0-1	859
0-2	886
180-1	2093
180-2	2109
100-1	2095
100-2	2179
60-1	2087
60-2	2062

Table B.3.4: Bond Strength data for Transpo T-48 with peel ply surface preparation.

Sample	Max Load (lbs)
1	890
2	1200
3	939

Table B.3.5: Bond strength data for E-Bond 526 sample.

Sample	Max Load (lbs)
0-1	798
0-2	806
180-1	1035
180-2	1044
100-1	863
100-2	792
60-1	816
60-2	829

Table B.3.6: Bond strength data for E-Bond 526 with peel ply surface preparation.

Sample	Max Load (lbs)
1	867
2	822
3	765

APPENDIX C

ASTM STANDARDS FOR POLYMERS AND POLYMER CONCRETE

C531-00	Standard Test Method for Linear Shrinkage and Coefficient of Thermal Expansion of Chemical-Resistant Mortars, Grouts, Monolithic Surfacings, and Polymer Concretes
C579-01	Standard Test Methods for Compressive Strength of Chemical-Resistant Mortars, Grouts, Monolithic Surfacings and Polymer Concretes
C881-02	Standard Specification for Epoxy-Resin-Base Bonding Systems for Concrete
C882-99	Standard Test Method for Bond Strength of Epoxy-Resin Systems Used With Concrete By Slant Shear
C884-98	Standard Test Method for Thermal Compatibility Between Concrete and an Epoxy-Resin Overlay
D570-98	Standard Test Method for Water Absorption of Plastics
D638-03	Standard Test Method for Tensile Properties of Plastics
D695-02	Standard Test Method for Compressive Properties of Rigid Plastics
D790-03	Standard Test Methods for Flexural Properties of Unreinforced and Reinforced Plastics and Electrical Insulating Materials
D2240-03	Standard Test Method for Rubber Property—Durometer Hardness
E524-00	Standard Specification for Standard Smooth Tire for Pavement Skid-Resistance Tests

APPENDIX D

CONTACT INFORMATION FOR POLYMER CONCRETE OVERLAY SUPPLIERS

Degadur Polymer Concrete

Contact: SRS, Röhm America L.L.C.
2 Turner Place, Piscataway, NJ 08855-0365
Phone: 800-477-4545 or 877-ROHMUSA (877-764-6872)
Fax: 723-981-5108 or 732-981-5484
Email: srs-information@degussa.com

General Description, http://www.roehm.com/rohmamerica/srs/products

Completed Projects, http://leadstates.tamu.edu/car/SHRP_products/2035b_degadur.stm

E-Bond 526 Multicoat Epoxy

Contact: E-Bond Epoxies, Inc.
P.O. Box 23069
Ft. Lauderdale, FL 33307
Phone: 954 566 6555
Fax: 954 566 6663
E-mail: info@ebondepoxies.com

General Description, http://www.ebondepoxies.com/epoxy-concrete.htm

Completed Projects, http://leadstates.tamu.edu/car/SHRP_products/2035B_ebond.stm

Poly-Carb Mark-163 FlexoGrid Flexible Epoxy-Urethane System

Contact: Poly-Carb, Inc
33095 Bainbridge Road
Solon, Ohio 44139 USA
Telephone: 440.248.1223
Toll-free: 800.CALL-MIX (225-5649) / 866-POLY-CARB (765-9227)
Fax: 440.248.1513
E-mail: info@poly-carb.com

General Description, http://www.poly-carb.com/

Completed Projects, http://leadstates.tamu.edu/car/SHRP_products/2035B_polycarb.stm

Pro-Poxy Type III DOT

Contact: Unitex
3101 Gardner
Kansas City, MO 64120
816-231-7700
800-821-5846
Fax: 816-483-3149

General Description, http://www.unitex-chemicals.com/catalog/propoxy_dot.shtml

Test Data, http://www.unitex-chemicals.com/testdata/propoxy_dot.html

Reichhold Polite 31280 (Unpromoted) / 32300 (Prepromoted)

Contact: Reichhold, Inc.
Research Triangle Park
NC 27709
(919) 990- 7500
Fax: +1 919 990 -7711

General Description, http://www.reichhold.com/prodbull/polylite 31830.pdf

Completed Projects, http://leadstates.tamu.edu/car/SHRP_products/2035b_reichhold.stm

Sikadur 22 Lo-Mod Epoxy Broadcast Overlay System

Contact: Sika Corporation
201 Polito Avenue
Lyndhurst, NJ07071
Phone: 800-933-7452
Fax: 201 933 6225
E-mail: sikainfo@sika-corp.com

General Description, http://www.sikaconstruction.com/tds-cpd-SikadurEpoxyOverlay.pdf

Completed Projects, http://leadstates.tamu.edu/car/SHRP_products/2035b_sikadur.stm

Tamms Flexolith Epoxy System

Contact: Tamms Industries, Inc.
3835 State Route 72
Kirkland, IL 60146
800-862-2667
info@tamms.com

General Description, http://www.tamms.com/

Completed Projects, http://leadstates.tamu.edu/car/SHRP_products/2035b tamms.stm

Transpo T-48 Epoxy Overlay System

Contact: Transpo-Industries, Inc.
20 Jones Street
New Rochelle, NY 10801
Phone: 914 636 1000
Fax: 914 636 1282
E-Mail: info@transpo.com

General Description, http://www.transpo.com/Transpo_Sheets_PDF/T-48_spec.pdf

Completed Projects, http://leadstates.tamu.edu/car/SHRP_products/2035b_transpo.stm